COO-3158-60

AN IN-SITU FIELD-ION MICROSCOPE STUDY OF THE RECOVERY BEHAVIOR OF HEAVY METAL ION-IRRADIATED TUNGSTEN, TUNGSTEN (RHENIUM) ALLOYS AND MOLYBDENUM

by

Charles H. Nielsen

Cornell University
Ithaca, New York 14853

Report #2942

Issued by

The Materials Science Center

Prepared for

THE U.S. DEPARTMENT OF ENERGY UNDER CONTRACT
No. EY-76-S-02-3158.*000

DISCLAIMER

Report #2942

COO-3158-60

AN IN SITU FIELD ION MICROSCOPE STUDY OF THE RECOVERY BEHAVIOR OF HEAVY METAL ION IRRADIATED TUNGSTEN, TUNGSTEN(RHENIUM) ALLOYS AND MOLYBDENUM

by

Charles Hart Nielsen

Ms Thesis
June 1977

Research Group:
Prof. D. N. Seidman
MSE

ACKNOWLEDGMENTS

The author expresses gratitude to his advisor, Professor David N. Seidman for his guidance and constant encouragement. The author wishes to thank Mr. Robert Whitmarsh, Mrs. Karen Pratt and Mr. B.F. Addis for their expert technical assistance. Appreciation is expressed to Dr. K.L. Wilson, Mr. A. Wagner, Dr. G. Ayrault, Dr. T. Hall and Mr. C.Y. Wei for their many helpful discussions.

This study was supported by the United States ERDA and by Cornell University Materials Science Center.

TABLE OF CONTENTS

LIST OF FIGURES

LIST OF FIGURES(continued)

LIST OF TABLES

AN IN SITU FIELD ION MICROSCOPE STUDY OF THE RECOVERY BEHAVIOR OF HEAVY METAL ION IRRADIATED TUNGSTEN, TUNGSTEN(RHENIUM) ALLOYS AND MOLYBDENUM

Charles Hart Nielsen, M.S.

Cornell University, 1977

ABSTRACT

Three field ion microscope (FIM) experiments were carried out to study the annealing behavior of heavy ion irradiated tungsten, tungsten (rhenium) alloys and molybdenum. The first experiment dealt with the stage I long-range migration of tungsten self interstitial atoms (SIAs) in high purity tungsten of resistivity ratio, $\mathcal{R} = 24{,}000$ ($\mathcal{R} = \rho_{300}/\rho_{4.2}$, where ρ_{300} and $\rho_{4.2}$ are the room temperature and 0°C resistivities). The FIM specimens were irradiated <u>in situ</u> at 18 K with 30 keV W^+ ions to an average dose of $5 \cdot 10^{12}$ ions cm^{-2} and subsequently examined by the pulsed-field evaporation technique. Several SIAs were observed to be immobile in the bulk of the specimen at 18 K. The high purity tungsten tips were also irradiated at 6 K to an average dose of $5 \cdot 10^{12}$ ions cm^{-2} and were allowed to isochronally warm at a rate of 2 K $min.^{-1}$. The surface of the specimen was continuously observed for extra bright-spots signaling the arrival of an SIA to the surface. By plotting the temperature dependence of the arrival rate of SIAs the long-range migration of SIAs was characterized. It was found that between 20 and 30 K the flux of SIAs arriving at the surface was much too high to be explained by a single thermally

activated process occurring at 38 K. The second experiment dealt with the phenomenon of impurity atom trapping of SIAs during long-range migration. It was shown that rhenium atoms in a tungsten matrix tend to capture tungsten SIAs and remain bound up to temperatures as high as 390 K. This was shown by irradiating tungsten-1 at.% rhenium and tungsten-3 at.% rhenium with 30 keV W^+ ions at 18 K to a dose of $5 \cdot 10^{12}$ ions cm^{-2} and observing the subsequent annealing behavior. It was expected that a major release peak would have been observed when the rhenium impurity atom-tungsten SIA complex dissociated. No such peak was observed up to 390 K and therefore it was concluded that the binding energy of the complex was at least 0.8 eV based on a simple diffusion model. An attempt to observe a tungsten-rhenium complex was made via the pulsed-field evaporation technique after a low temperature (18 K) irradiation followed by an anneal to 400 K. Several complex-contrast effects were observed in the bulk of the specimen and were considered to be tunsten-rhenium complexes. The final experiment was concerned with the low temperature annealing kinetics of irradiated molybdenum. High purity molybdenum of resistivity ratio $\mathcal{R} = 5700$ was irradiated at 10 K with 30 keV Mo^+ ions to a dose of $\sim 5 \cdot 10^{12}$ ions cm^{-2}. The annealing spectrum revealed a series of peaks the largest of which was centered at 32 K. Theoretical analysis of this peak suggested that, unlike the tungsten peak, it could represent the single thermally activated process associated with the onset of long-range migration. A study of the effect of the large electric field required for field ionization on the diffusivity of the molybdenum SIA was made by comparing the spectra of specimens irradiated at 10 K in the absence of an electric field with identical specimens irradiated at 40 K and cooled to 10 K in the absence of an electric field. The results indicated that

the electric field has only a minimal effect on the SIA annealing kinetics. This tends to strengthen the contention that the molybdenum SIA becomes mobile at 32 K.

1. INTRODUCTION

1.1. Motivation

The primary objective of this study was to observe the annealing behavior (recovery) of the stage I self-interstitial atom (SIA) in tungsten and molybdenum utilizing field ion microscopy (FIM). The recovery of SIAs introduced into metals by heavy-ion irradiation is of interest to the materials scientist in that these defects have pronounced effects on the mechanical properties of materials.[1] Thus an understanding of the recovery temperature regimes and the corresponding recovery mechanisms for these defects is desirable. In particular, knowledge of the temperature, and even more fundamentally the existence, of the stage I long-range migration region is important since it determines the nature and amount of damage remaining at higher temperatures.

Further motivation is provided by the fact that there exists a fair amount of controversy in the literature concerning the recovery temperature regime of tungsten and molybdenum SIAs and the mechanisms by which they recover. The SIA has been reported to become mobile at several temperatures ranging between 15 to 77 K in tungsten and 25 to 60 K to not at all in molybdenum based primarily on electrical resistivity and internal friction experiments. The debate over the mechanisms of recovery in general has been split into two schools of thought characterized by the one-interstitial model[2] versus the two interstitial model.[3] Another debate, much larger in scope, centers on the question of the analogy between the relatively well understood recovery processes occurring in FCC metals and the less understood recovery of BCC metals.

With the advent of FIM, the ability to directly observe atomistic

processes involved during recovery was first realized. As early as 1964, Sinha and Muller[4] had reported direct evidence of interstitial migration in tungsten in the temperature range of 50 to 90 K by means of FIM observations. However, the inability to accurately measure the FIM tip temperature hampered the quanitative capability of these early studies. Galligan[5] avoided this problem by examining the lattice isothermally using the field-evaporation technique after irradiation at temperatures below and above stage II. Then by determining the concentrations of observed defects before and after recovery he was able to assign mechanisms to the process. This technique had the drawback that often two types of defects (usually vacancies and SIA complexes) were observed to disappear during the recovery. Hence, one could not unambiquously determine which defect became mobile during the recovery stage.

The first isochronal FIM study of the recovery behavior of in-situ irradiated tungsten was reported by Scanlan, Styris and Seidman[6] in 1971. A technique was developed whereby the tip temperature could be accurately recorded while continuously photographing the surface of the tip. They recorded the appearance of extra bright-spots at the surface as a function of temperature and concluded that they were observing mobile SIAs. It was shown by Scanlan et al. by fitting the data to a simple diffusion model that they had in fact observed the onset of long-range migration. Later, Wilson and Seidman[7] reported that the FIM recovery spectra of tungsten doped with carbon contained what was identified as a detrapping peak. Recently, Wei and Seidman[8] have observed the stage II detrapping peak in the FIM isochronal recovery spectrum of dilute platinum (gold) alloys.

The above experiments have shown that the FIM technique provides the capability to observe isochronal recovery on an atomistic level. Thus it

is now possible to identify, unambiguously, the temperature range in which recovery processes involving SIA long-range migration occur and perhaps the mechanisms by which they occur. Furthermore, the combination of FIM isochronal recovery spectra and FIM isothermal pulsed-field evaporation allows one to examine recovery processes involving SIA clusters, SIA-impurity clusters and vacancies.

The purpose of this thesis was three fold: first, the annealing behavior between 6 and 35 K in pure tungsten was examined for small amounts of recovery below the dominant 38 K peak in the FIM recovery spectra (this had become necessary in light of recent experimental results which were in conflict with the results of Scanlan et al.); second, the thermodynamics of impurity trapping of the SIA in dilute tungsten-rhenium alloys during stage I recovery was examined in the form of an FIM search for an impurity-SIA release peak; and finally, a systematic FIM investigation of stage I and II recovery in molybdenum was performed.

1.2. Experimental Apparatus

The experimental equipment consisted of a Hill-Nelson type sputtered-metal ion-source connected to an ultra-high vacuum field-ion microscope (FIM) by a three-stage differentially pumped flight-tube. For further details regarding the ultra-high vacuum FIM, the heavy metal-ion accelerator, the cryogenic technique, the temperature measurement and the semi-automatic data recording and analysis system see Scanlan et al.[6] and Wilson.[9]

1.3. Experimental Details

1.3.1. Specimen Preparation

Tungsten and molybdenum specimens were electropolished to an initial FIM tip radius of ~200 A from either 0.025 cm diameter thinned single crystals or 0.01 cm diameter polycrystalline wires. Two basic methods of tip making were employed: the ac dipping and dc drop-off techniques.

1.3.1.1. The ac Dipping Technique for Polycrystalline Specimens

In the ac dipping technique the 0.01 cm diameter polycrystalline wire was suspended vertically 4 mm into the electrolyte (1N NaOH aqueous solution for W and W-Re alloys and a solution of 1 part H_2SO_4 to 10 parts MTOH for Mo) and a 4.2 Vac potential was applied between the specimen and a stainless steel electrode. The end of the specimen polished more rapidly thus creating a natural taper. The electropolishing was terminated when 2 mm of the wire had been removed. The tip was then examined in an optical microscope at 100X for any large deformations and, if acceptable, was then mounted in the specimen holder of the FIM. A tip made in such a fashion typically imaged between 3 and 4 kV potential for tungsten and between 2 and 3 kV potential for molybdenum. This technique worked well for polycrystalline samples but proved to be unreliable for single crystals.

1.3.1.2. The dc Drop-Off for Single Crystals

In the dc drop-off method the thinned single crystals were first dipped 0.5 mm into a solution of Microstop (manufactered by Fisher Scientific Co., Rochester, N.Y.) and acetone. This effectively coated the end of the crystal such that it would resist electropolishing. The sample was then

immersed vertically 4 mm into the electrolyte (solutions identical to the ac dipping technique were used) and a 9 Vdc potential was applied to the specimen (anode) with respect to the stainless steel cathode. Approximately one minute of electropolishing produced a taper which went from a maximum at the air electrolyte interface to a minimum at the metal-Microstop interface. The 0.5 mm of material protected by the Microstop was unaffected and maintained its original diameter. The tip was then dipped 4 mm into acetone such that the coating of Microstop was completely dissolved. Then the tip was placed back into the electrolyte and the taper was allowed to propagate. The lower section of the tip (below the neck) was reduced in size by cutting it at the air-liquid interface. Before the lower section of the wire dropped-off the voltage was switched to 9 Vdc pulses 0.1 msec in duration. These pulses were terminated immediately upon observation of the drop-off. A desirable aspect of this technique was that the tip could be re-formed without considerable loss of material. Therefore, if upon examination in the FIM, the endform was found to be too blunt or plastically deformed, it could be dropped-off again forming another tip with a loss of only 0.5 mm of material.

1.3.2. Development of Final End Form

Both ac dipped and dc dropped-off tips were quite rough on an atomic scale. The development of an atomically smooth end form was carried out via dc field evaporation followed by pulsed-field evaporation. Pure tungsten and molybdenum tips were developed in a static pressure of $3 \cdot 10^{-5}$ torr (guage pressure are used reported throughout this thesis) helium at a temperature of 300 K for tungsten and 77 K for molybdenum. The tungsten (rhenium) alloys were developed in a static pressure of $3 \cdot 10^{-5}$ torr neon at a temperature of 300 K. Both the neon and helium image gas supplied

were Matheson assayed grade (99.995% pure) contained in a 1 liter glass flask which was cryo-pumped at 77 K with liquid nitrogen. The neon gas supply was changed every two months and the helium gas supply every six months to assure low impurity levels.

In both cases the dc voltage was slowly increased until an image appeared. The speed at which the potential was then incremented depended upon the evaporation rate of the imaged atoms. Usually upon obtaining a 7 KV image the dc voltage could be safely increased in 200 V steps every 5 minutes until the image filled the entire screen.

1.3.3. Experimental Procedure

Upon obtaining a suitable end form the specimen was cooled to the irradiation temperature (T_o) and adjusted to the proper best image voltage (BIV). The irradiation was carried out in-situ in the absence of the electric field and image gas at the desired irradiation temperature. The total dose was accurately measured by a Faraday cage placed behind the specimen. The background pressure was maintained at $1 \cdot 10^{-9}$ torr or less. Typically the irradiation was completed within 15 minutes so that the specimen surface remained clean during the course of an irradiation. The imaging gas was then admitted dynamically into the FIM via a Varian leak value to a pressure of $1 \cdot 10^{-5}$ torr and the specimen returned to BIV. The beam side of the tip showed the effects of the irradiation in the form of a sputtered surface; see Wilson and Seidman[7] for an example. The surface damage was then removed by the pulsed-field evaporation of at least 10 A of material.

One of two types of experiments was then performed; namely either an atom-by-atom dissection of the lattice or an isochronal anneal. The atom-

by-atom dissection (or peel) of the crystal was carried out by subjecting the tip to controlled pulsed-field evaporation. The semi-automated system[9] took a photograph of the surface between successive pulses, thus recording each crystal layer as it was field evaporated. The film was then scanned on a Vanguard motion analyzer for the appearance of additional bright-spots (SIAs or impurity atoms) or any vacant lattice sites. For an isochronal anneal the specimen was warmed isochronally at $\sim$2 to 3 K min^{-1} while the ciné camera photographed the surface continuously at 0.4 frames sec^{-1}. The temperature was measured by a platinum resistance thermometer (PRT) and was recorded by correlating the 24 hour accutron clock and frame counter on each frame of film. The ciné film depicting the annealing behavior was analyzed for the appearance of extra bright-spots at the surface which signaled the arrival of SIAs.

1.3.4. The Damage State

It is essential in the analysis of annealing behavior to be aware of the state of damage in the specimen produced by the irradiation species. For the case of heavy metal ions, specifically W^+ ions, it has been shown[8] that in an energy range of 20 to 30 keV depleted zones are produced in tungsten at a depth of $\sim$ 20 to 100 A below the irradiated surface. These zones consisted of a vacancy-rich core ($\sim$10 at.%) surrounded by a mantle of SIAs ($\sim$1 at.%) as well as a number of SIAs which were separated from the depleted zones by a distance of $\sim$50 to 150 A at 18 K.[10] These latter SIAs were produced by the focused replacement collision sequence mechanism.

2. LONG-RANGE MIGRATION OF TUNGSTEN SIAs

2.1. Review of Literature

As mentioned earlier the study of long-range migration has primarily been carried out by indirect experiments. The vast majority of these have employed the electrical resistivity and internal friction techniques. The assignment of an atomic mechanism to a particular recovery stage thus involved deriving atomistic properties from the annealing behavior of macroscopic properties. This involves several assumptions concerning the damage state and is at best a "black box" type measurement. For a review of experiments on stage I recovery in tungsten and an indication of the degree of controvery on the subject prior to 1970 see Schultz[11] and Moser[12].

It has been established[6] that the FIM technique is ideally suited for directly identifying the atomic mechanism responsible for a given recovery stage. Furthermore, information concerning the migration energy and possibly configuration can, in principle, be deduced from FIM data. The first attempt at discerning the annealing behavior of the tungsten SIA with field-ion microscopy was made by Müller and Sinha[4] in 1964. They reported the appearance of extra bright-spots at the surface for a few seconds after an irradiation by 20 keV helium ions at 21 K. It was suggested that these were SIAs close to the surface whose activation energy for diffusion had been lowered by the external field. During the subsequent anneal they observed a few interstitials arriving at the surface near 50 K, several around 90 K and none above 100 K. However, difficulties in measuring the true tip temperature were encountered and a more complete study was never performed by these authors.

The most comprehensive FIM study of the long-range migration of the SIA in pure tungsten, to date, was reported by Scanlan, Styris and Seidman[6, 13] in 1971. The annealing spectrum of pure tungsten irradiated at either 8 or 16 K by 20 keV W^+ ions showed that the majority of the SIAs ($\sim$40%) appeared between 27 and 42 K with a maximum at $\sim$38 K. Since only SIAs which have made $\sim 10^4$ jumps can be detected by the FIM, the 38 K peak was interpreted as the onset of long-range migration. The diffusion of an SIA in an FIM tip via a single thermally-activated process was then mathematically modeled and fit to the 38 K peak. This analysis yielded an enthalpy change of migration (Δh^m_{1i}) equal to 0.085 eV. However, concern was expressed for the effect that the external electric field had on the diffusivity of the SIA; i.e., it was not clear in the expression $\Delta u^m_{1i} = \Delta h^m_{1i} + p\Delta v^m_{1i}$ that the $p\Delta v^m_{1i}$ term could be neglected in the special case of diffusion in an FIM tip. If the negative hydrostatic pressure created by the imaging electric field was large enough to significantly reduce Δh^m_{1i} then the diffusivity of the SIA would have been increased. However, it was shown by Scanlan et al. that the $p\Delta v^m_{1i}$ term could be measured by a series of experiments and that an upper limit could be placed on the Δv^m_{1i} .

The next significant contribution to the problem of assigning atomistic mechanisms to recovery stages in tungsten using the FIM was the evaluation of Δv^m_{1i} for tungsten by Wilson and Seidman.[7] By comparing the isochronal recovery spectra of pure tungsten irradiated at 18 and 50 K they were able to show that tungsten SIAs were mobile at 50 K in the absence of the imaging electric field. This suggested that if the onset of long-range migration occurred at 50 K in the absence of the electric field and at 38 K in the presence of the electric field then only a

peak shift of ~12 K was possible. The corresponding reduction in energy could then be calculated employing a linear relationship between the activation energy of the recovery process (Q) and T_m. This was shown to be given by $Q(eV) = 2.24 \cdot 10^{-3}$. T_m for tungsten. The value of Δv_{1i}^m was then obtained by equating this energy change to $p\Delta v_{1i}^m$ or equivalently $(E^2/8)\Delta v_{1i}^m$. Here, E is the electric field required for field ionization of the helium imaging gas and has been shown to be equal to ~4.75 VA^{-1}. The above calculation resulted in an upper limit to Δv_{1i}^m of 0.02 atomic volumes (Ω_a)*. It was noted that for $\Delta v_{1i}^m = 0.02\,\Omega_a$ and an evaporation field of 6 VA^{-1} that the ratio of the SIA diffusivity during pulsed-field evaporation at 18 K to the SIA diffusivity while imaging at 38 K was 10^{-9}. Since the evaporation field was applied to the specimen for a total of only ~10 sec during the pre-anneal peel it was concluded that no significant SIA migration could have occurred due to the experimental conditions before the anneal. Clearly it is the extremely small value of Δv_{1i}^m that has minimized the effects of the external E on FIM results.

The effects of impurity content on the FIM isochronal annealing spectrum were also studied by Wilson and Seidman[9]. Five different purity levels of tungsten, along with two tungsten(rhenium) alloys and carbon doped tungsten received in-situ irradiation followed by isochronal anneals. It was found that the four highest purity tungsten specimens exhibited essentially the same basic recovery spectrum; a series of distinct recovery peaks at 38, 50, 65 and 80 K. The resistivity ratio ($R = R_{300K}/R_{4.2K}$) ranged from $5 \cdot 10^4$ to 15 yet only minor variations were seen in the FIM isochronal

* The value of Ω is $a^2/2$ for a BCC lattice, where a is the lattice parameter.

recovery spectra. The $R=5$ tungsten spectrum lacked the sharp peak structure found above 45 K in the purer specimens, but the dominant 38 K peak was still present.

The tungsten-3 at.% rhenium alloy showed almost no isochronal recovery over the entire range from 18 to 120 K. The tungsten-0.5 at.% rhenium exhibited strongly reduced isochronal recovery, relative to pure tungsten, between 18 and 120 K; in addition, the long-range migration peak appeared between 30 and 35 K. This downward shift in the peak temperature (T_m) with increasing impurity atom concentration had been predicted by Seidman[14]. In the case of the tungsten(carbon) alloy the peak at 38 K was diminished by $\sim$20% and the peak at 50 K was enhanced. It was suggested that this constituted evidence for the formation of SIA-carbon complexes in stage I and the subsequent release of SIAs from the carbon atoms in substage II_A ($\sim$50 K).

The above experiments led Seidman and co-workers to conclude that for the unalloyed tungsten the SIAs only interacted rather weakly with impurity atoms and that SIA-SIA interactions dominated the recovery behavior above 45 K. This was considered to be the result of the fact that the SIA concentration in the local vicinity of a depleted zone is $\sim$1 at.%, while the average impurity atom concentration is much less than 1 at.%.

Recently, it was reported by Wilson[9] that the above scheme was corroborated by preliminary dose dependence experiments. Isochronal anneals were performed on tungsten irradiated at 18 K to an order of magnitude higher dose. The results exhibited a suppression of the 38 K peak and an enhancement of the 50 K peak. This was explained as evidence for increased SIA cluster formation during long-range migration at 38 K and increased SIA cluster migration at 50 K.

Several isochronal recovery experiments, other than FIM, carried out concurrently with the FIM work of Seidman and co-workers corraborate the existence of long-range migration in tungsten below 45 K. It should be noted here that electrical resistivity measurements can detect long-range migration of SIAs only by altering a given parameter and comparing the resulting isochronal spectrum with the standard one. Typically, it is the sink structure of the material that undergoes the deviation from standard state.This is accomplished usually by either seeding specimens with vacancies, doping them with impurity atoms or varying the irradiation dose. It is expected that if a given recovery peak is associated with long-range migration then: (1) it will become enhanced by the presence of additional vacancies; (2) it will be surpressed and shifted to higher temperatures due to trapping at impurity atoms or; (3) it will shift to lower temperatures with increasing dose.

For example, Kunz, Faber, Lachenmann and Schultz[15] reported that the effect of quenched-in vacancies on the recovery spectra of electron irradiated tungsten was to enhance the substages at 28 and 40 K. Klabunde et al.[16] showed that for thermal neutron irradiated tungsten there existed dose dependent stages at 21, 27, and 80 K. Furthermore, Dausinger, Schultz, Boning and Vogl[17] reported that impurity doping of electron irradiated tungsten tended to surpress the 40 K recovery stage and extensively change the peak structure above this temperature. The above results were interpreted by each investigator to indicate that long-range migration of the SIA occurs below 45 K.

More recently two additional studies have been published which verify the mobility of the SIA below 45 K, but assign much lower peak temperature to the phenomenon than the 38 K reported by Scanlan et al. Firstly, Okuda

and Mizubayashi[18] measured the internal friction and dynamic modulus of tungsten oriented single crystal ($\mathcal{R}$ = 8200) after neutron-irradiation near 4.2 K. They observed two pronounced dislocation pinning stages at 15 and 30 K where the internal friction decreased and the dynamic modulus increased. Their data was interpreted to imply that the long-range migration of a 110 split SIA was responsible for the pinning stage at 15 K and that the stage at 30 K was due to the detrapping of SIAs from impurity atom traps. Okuda and Mizubayashi contend that the FIM results of Scanlan et al. are not contrary to their work because the irradiations of the FIM specimens were performed in a temperature range where the SIA was already mobile and thus, the 38 K peak in the FIM isochronal recovery spectra could be attributed to the dissociation of SIAs from impurity atom traps.

Secondly, Dausinger and Schultz[19] have recently presented the results of their dose dependence studies of the isochronal recovery behavior of tungsten. They found recovery peaks at 11, 17, 27, 30.5, 38 and 43 K in high purity tungsten ($\mathcal{R}$ = 70,000) electron-irradiated to a close-pair concentration of 25 appm. It was observed that only the substage between 24 and 30 K shifts to lower temperatures with increased pair concentration (i.e., dose). The peak shift indicated that the number of jumps required for the SIA to recover had decreased as a result of an increased concentration of vacancies. Thus, Dausinger and Schultz ascribed this substage to uncorrelated long-range migration. They suggest that their data can be considered to be in agreement with that of Scanlan et al. if their FIM peaks are shifted to lower temperatures by 5 to 6.5 K.

Thus it is clear that for tungsten there remains a large degree of uncertainly concerning the completion temperature of stage I, or equivalently, the onset of uncorrelated long-range migration of the SIA. It is

the purpose of this chapter to present work done to check the FIM data of Seidman and co-workers, specifically the careful extension of the isochronal anneals to as low as irradiation temperature as possible. In addition, the results of a search for immobile SIAs at 20 K via the pulsed-field evaporation technique will be presented. Finally, the interpretation of the experiments will be discussed with respect to those of Okuda et al., Dausinger et al., and others.

2.2. Additional Experimental Details

Commercially pure tungsten in the form of 20 cm long rods with initial diameters of 1.5 mm were obtained from Westinghouse. Oriented single crystals were then grown from the Westinghouse tungsten by passing an electron-beam molten zone, having a maximum width of less than 1 cm, from the bottom (seed end) to the top of the rods. Each crystal received was thinned to 0.5 mm diameter by dc electropolishing at 30 volts in a solution of 20 g NaOH in one liter of a 60-40 mixture of glycerol and water with air bubbled through the electrolyte. A 4 cm section of each crystal was then removed and tested for purity by measuring its resistivity ratio. A value of $R = 2.4 \cdot 10^4$ (uncorrected for size effects) was obtained for the two-pass zone-refined single crystal used in our experiments. The remaining material was polished and sectioned into 1.5 cm lengths of typically 0.1 mm diameter in a 1 N NaOH electrolyte at 9 Vdc. The sections were then polished into FIM tips by the dc drop-off technique (see section 1.3.1.).

2.3. Results

2.3.1. Pre-Anneal Pulsed-Field Evaporation Experiments at T_o

Pulsed-field evaporation experiments were carried out on four different specimens with $\mathcal{R}$ = 24,000 at T_o = 20 K. The object of these experiments was to establish the existence of immobile SIAs in the bulk of the specimen at T_o. The results of the pre-anneal pulsed-field evaporation experiments are given in Table 1. A plot of the atomic concentration of SIAs as a function of the dose is displayed in figure 1. It is clear that the concentration of SIAs increased linearly with heavy metal ion dose over the range investigated. Contrast patterns characteristic of SIAs were counted only on the {111}, {332}, {221} and {334} type planes. These planes were chosen because all of the inside atoms in the plane were clearly visible. A total of $1.77 \cdot 10^5$ inside atoms were counted and 25 unambiguous SIA contrast patterns were observed. This yielded an average SIA concentration of $1.4 \cdot 10^{-4}$ atom fraction. Figure 2 represents a typical evaporation sequence of a {111} type plane which includes a tungsten SIA.

The vital result established by the above experiments was that SIAs are immobile at the irradiation temperature. The fact that the SIAs are immobile at T_o while imaging the specimen shows that the imaging electric field had not caused a stress induced migration of these defects.

PLANE TYPE	RUN #1		RUN #2		RUN #3		RUN #4	
	ATOMS COUNTED	SIAs OBSERVED	ATOMS COUNTED	SIAs OBSERVED	ATOMS COUNTED	SIAs OBSERVED	ATOMS COUNTED	SIAs OBSERVED
111	$0.8 \cdot 10^4$	1	$1.9 \cdot 10^4$	0	$1.2 \cdot 10^4$	0	$0.7 \cdot 10^4$	1
433	$1.8 \cdot 10^4$	3	$2.8 \cdot 10^4$	0	$3.6 \cdot 10^4$	0	$1.4 \cdot 10^4$	3
332	$2.7 \cdot 10^4$	3	$2.1 \cdot 10^4$	1	$2.2 \cdot 10^4$	1	$2.2 \cdot 10^4$	4
211	$2.1 \cdot 10^4$	3	$1.0 \cdot 10^4$	0	$1.7 \cdot 10^4$	1	$1.8 \cdot 10^4$	4
TOTAL	$7.4 \cdot 10^4$	10	$7.8 \cdot 10^4$	1	$8.7 \cdot 10^4$	2	$6.1 \cdot 10^4$	12

Table 1

Summary of pulsed-field evaporation experiments on high purity tungsten irradiated at 18 K.

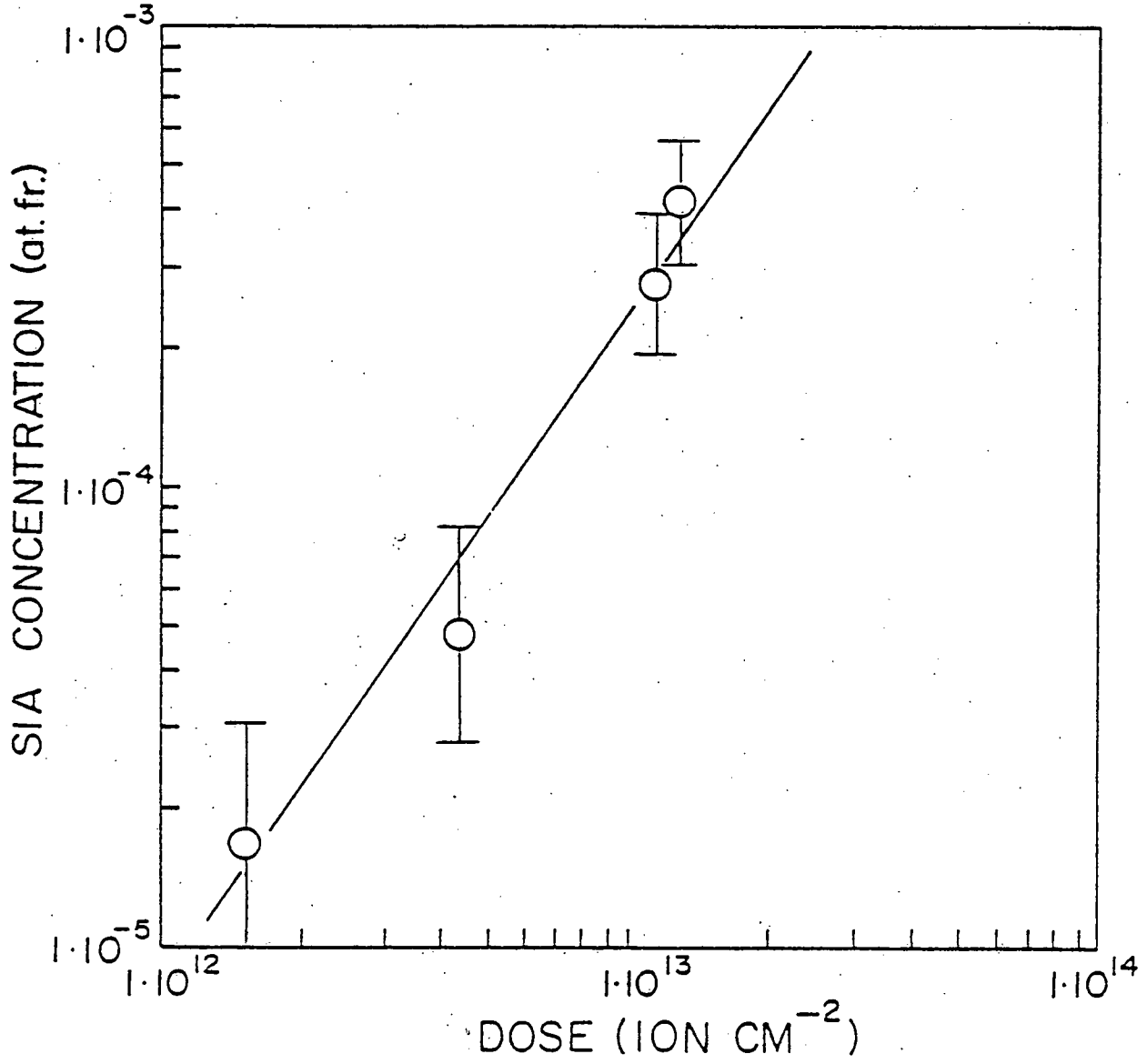

Figure 1. A plot of the atomic fraction of self-interstitial atoms as a function of ion dose. The incident energy of the W^+ ion irradiation was 30 keV at an irradiation temperature of 20 K. It is seen that the concentration of SIAs increased with ion dose over the range investigated.

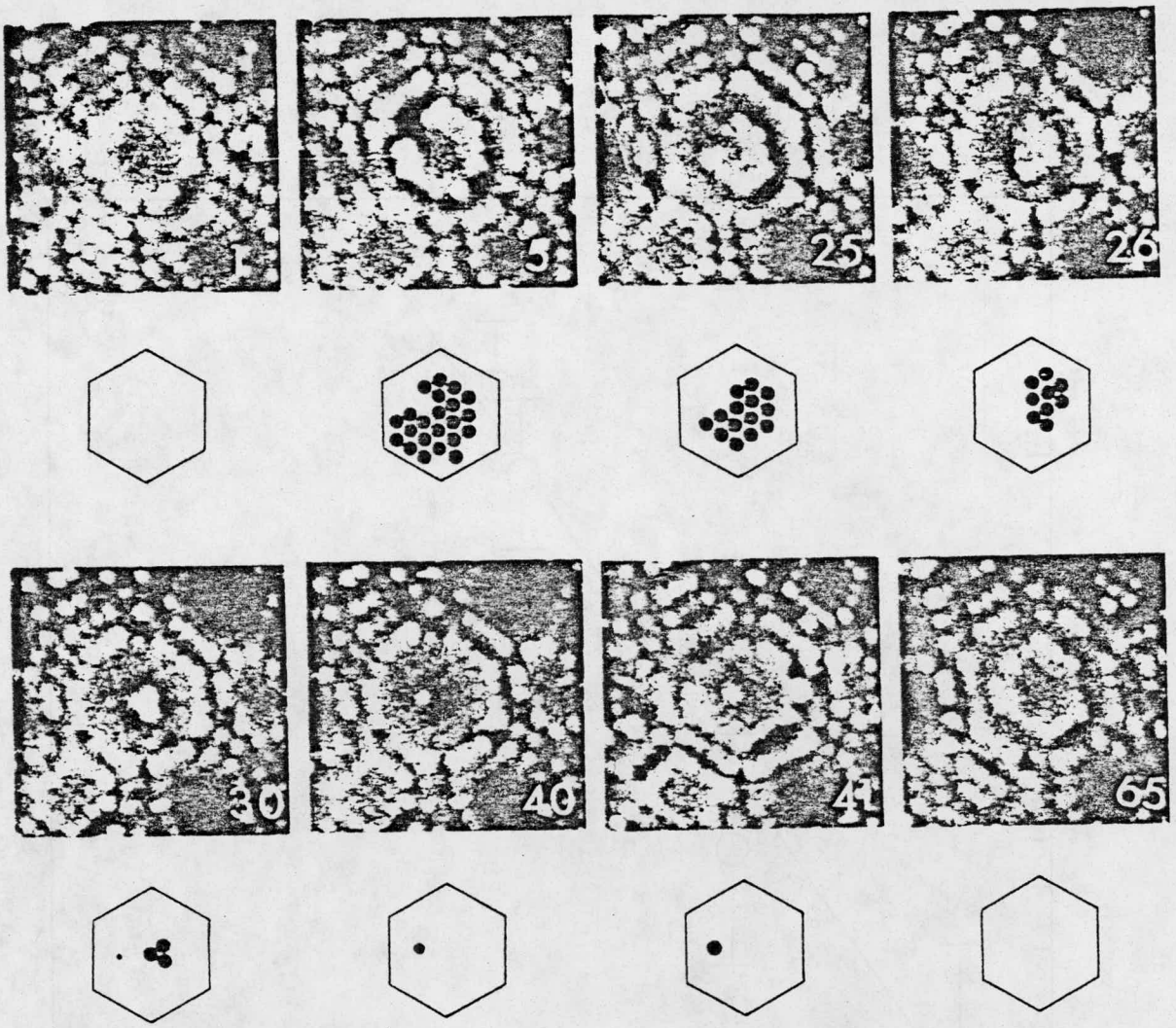

Figure 2. A series of 8 micrographs showing an SIA in the (111) plane of tungsten irradiated at 18 K. The number on the micrograph refers to the frame number on the cine film. Intermediate frames were omitted for clarity. The plane is illustrated below each micrograph. Frame 1 depicts a full plane which upon evaporation revealed one vacant site in frame 5. Frames 25 and 26 show the evaporation of the plane around the vacancy. Frame 30 shows the first appearance of an extra bright-spot. The extra bright-spot in fully imaged in frame 41 and evaporated in frame 65.

2.3.2. Continuous Annealing Behavior Between 6 and 120 K

High purity tungsten ($\mathcal{R} = 2.4 \cdot 10^4$) specimens in the form of FIM tips were irradiated *in situ* at 6 K to a standard dose of $5 \cdot 10^{12}$ W^+ ions cm^{-2} in the absence of an imaging gas. The gas was then reintroduced and the tips were isochronally warmed at a rate of $\sim$2 K min^{-1}. The surface of the tip was continuously monitored for the appearance of extra bright-spots. Each event was recorded photographically and was assumed to represent the arrival of an SIA to the surface. A histogram of the fraction of the total number of events per 5 K temperature interval is displayed in figure 3. The peak structure is seen to be in basic agreement with that obtained by Scanlan et al. and by Wilson and Seidman: namely a dominant recovery peak at 38 K followed by several peaks of diminishing magnitude. The 38 K peak has been interpreted by these workers as representing the onset of long-range migration of tungsten SIAs. The remainder of the spectrum must therefore be associated with stage II phenomena and most probably represents the continuous growth* of SIA clusters.(9) There exists, however, an important difference between the spectrum reported here and that reported by Scanlan et al. and Wilson and Seidman. This discrepancy lies in the leading edge of the 38 K stage and appears as a shoulder on the low temperature side of the peak. This feature of the annealing spectrum can be seen more clearly by analyzing the shape of the major 38 K peak. To accomplish this the data has been replotted as the number of events observed per 2.5 K interval and shown in figure 4. Since the high temperature side of the 38 K peak is overlapped

---

* Large SIA clusters can grow at the expense of small SIA clusters; this process requires the dissociation of the smaller clusters and the subsequent migration of SIAs to the larger cluster.

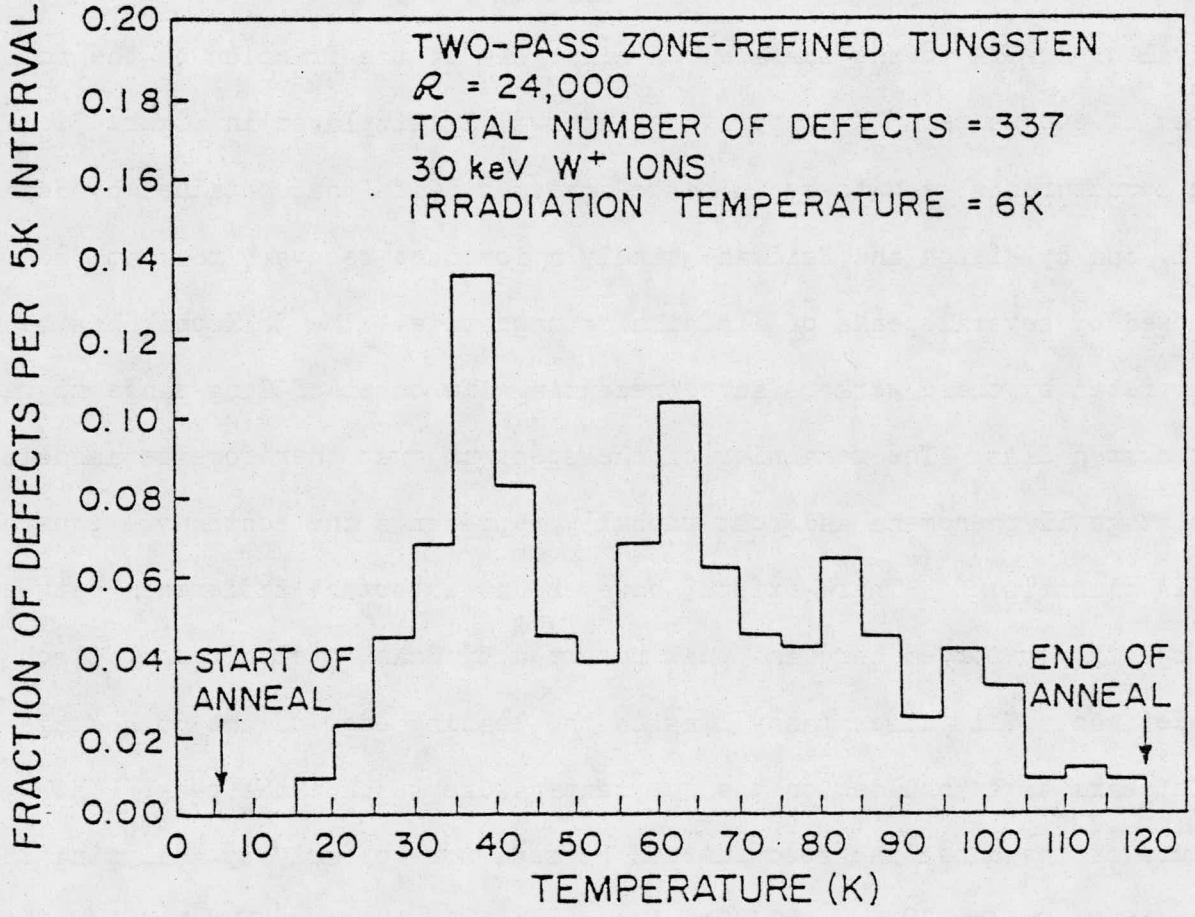

Figure 3. A composite isochronal annealing spectrum for four-pass zone-refined tungsten irradiated at 6 K with 30 keV W^+ ions and annealed to 120 K with a 2 K min^{-1} warming rate.

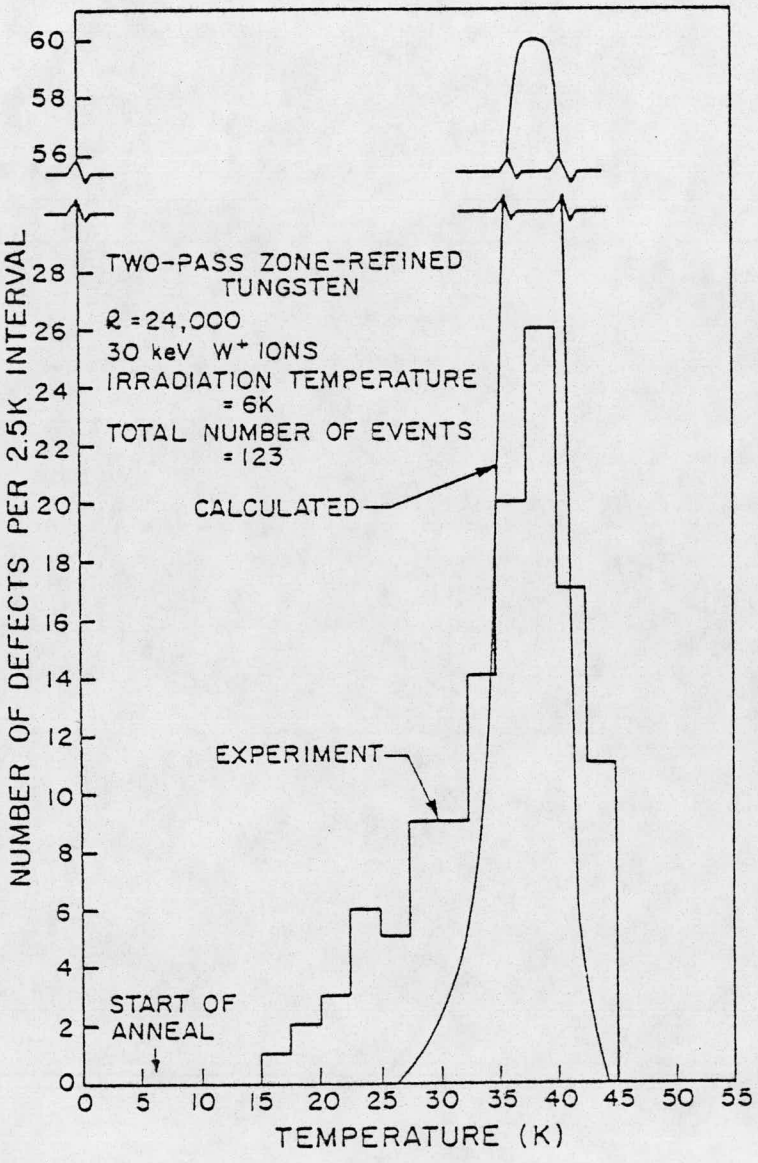

Figure 4. A composite isochronal annealing spectrum for four-pass zone-refined tungsten plotted with 2.5 K temperature intervals. Only the SIA events below 45 K are included in this histogram. A calculated isochronal annealing spectrum for a single thermally activated defect is superimposed on the experimental results. The theory of Scanlan et al.(6) predicted a peak temperature given by:

$$T_m = \Delta h_{1i}^m / k \cdot (\ln\Gamma - 2\ln\ln\Gamma)$$

with

$$\Gamma = \pi^2 D_{1i} \Delta h_{1i}^m / R^2 \alpha k$$

where R was the tip radius and α was the warming rate.

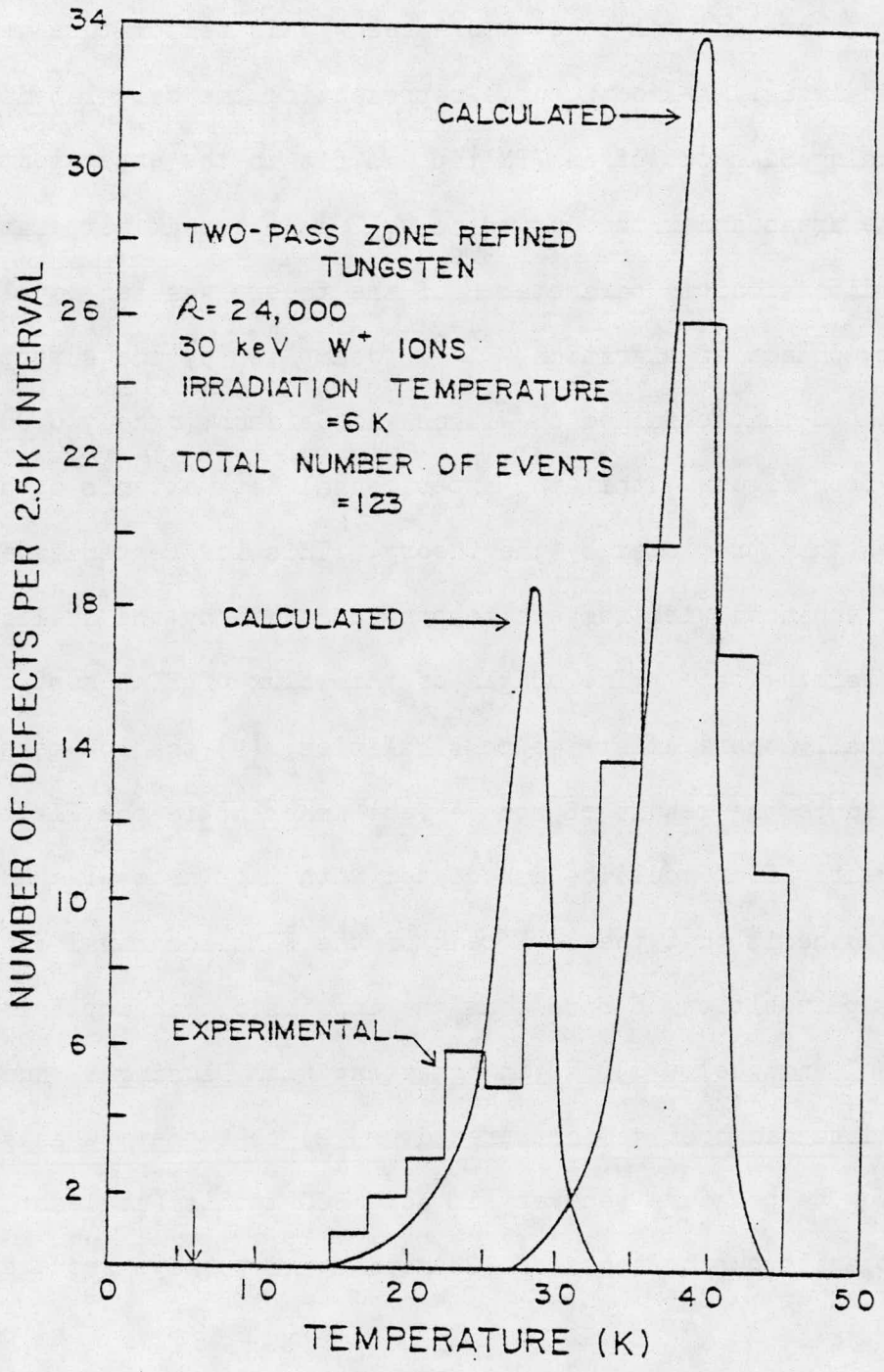

Figure 4a. The same experimental histogram as shown in figure 4 but with two calculated curves superimposed on the data. The sum of the area under the calculated curves is equal to the area under the experimental curve.

by the peak centered at 60 K, it is impossible to unambiguously determine the temperature at which stage I terminates. Therefore 45 K was assigned as a cut-off temperature and only the events below this temperature were included in the analysis. A smooth curve representing the calculated flux of randomly diffusing SIAs out of an FIM tip was fit to the experimental histogram such that the areas under the curves as well as the peak temperatures were equal. The dimensionless parameter Γ of the theory was set equal to 10^{16}. The enthalpy change of migration(Δh^m_{1i}) implied by the superposition was identical to that obtained by Wilson and Seidman; namely 0.085 eV.

It is clear from figure 4 that the experimental data extends to much lower temperatures than predicted by the theory. This low temperature recovery has been enhanced with respect to previous data by the utilization of a much slower warming rate. The origin of this flux of SIAs must now be considered. Basically there exist two possibilities: (1) the low temperature shoulder could be the result of some effect inherent in the FIM technique;or (2) the early flux could be associated with intrinsic SIA annealing behavior. The hypothesis that the 38 K peak of the FIM isochronal annealing spectrum is the superposition of more than one intrinsic peak implies that either: (1) stage I ends below $\sim$30 K (in agreement with Dausinger) and that the previous FIM data had been misinterpreted;or (2) that the mechanisms responsible for low temperature recovery in some BCC metals (at least tungsten) are not analogous to those of FCC metals and perhaps requires another defect.

In the two previous studies made on the FIM annealing behavior of low temperature irradiated tungsten[6,9], small amounts of recovery were found at temperatures below that predicted by the theory. This deviation from ideal behavior was considered inherent to the FIM technique and to be the

result of enhanced SIA diffusivity in the region just below the surface. The SIAs originally positioned only a few atom layers below the surface would therefore have become mobile at a lower temperature than the bulk SIAs and would appear at the surface earlier. This model was suggested by the calculations of Beeler[20] which showed that the activation barrier to migration was significantly less than the bulk value for the first few layers below the surface. However, there is yet to be experimental evidence published that would support such behavior.

Let us now consider the possibility that the major peak centered at 38 K represents the superposition of at least two intrinsic processes. To illustrate this point the experimental FIM isochronal recovery data shown in figure 4 has been replotted and fit with two calculated curves in figure 4a. The fit was made such that the areas under the two calculated curves equalled the area under the experimental peak. Each smooth curve represents a flux of randomly migrating SIAs to the surface of an FIM specimen as calculated by Scanlan et al.[6] and imply enthalpy changes of migration (Δh^m_{1i}) of 0.058 eV for the peak centered at 26 K and 0.085 eV for the peak centered at 38 K. In order to explain these peaks one must recall that both peaks involve long-range migration and are insensitive to impurity concentrations of less than $\sim$1 at.%. Considering the above restrictions at least two possibilities exist which would explain the appearance of two long-range migration peaks below 45 K. Firstly, it is reasonable to assign the onset of long-range migration to the smaller peak (at 26 K) and describe the larger peak (at 38 K) as the dissociation or migration of SIA-SIA pairs. It has been reported[10] that since there is such a high local concentration of SIAs around the depleted zones, SIA-SIA

interactions are dominant. A small fraction of the SIAs would complete the journey to the surface without interacting with another SIA, thus producing the minor peak at $\sim$30 K. The remaining SIAs would have become immobilized upon forming SIA-SIA pairs. These larger defects would then become mobile (or perhaps dissociate) near 38 K and complete their journey to the surface. The strength of this theory depends on the non-random initial distribution of SIAs in the bulk and also on a small but significant binding energy between single SIAs. This argument seems to be in agreement with the results of Dausinger and Shultz where long-range migration was observed near 28 K.

Secondly, there exists the possibility of another as yet unknown defect produced in addition to simple Frenkel pairs. The character of such a defect is impossible to determine from the existing experimental data. Afman[21] has proposed a model for the recovery of electron irradiated molybdenum which requires the existence of a new defect. This defect would, according to Afman, be extended (made up of one half SIA and one half vacancy) and could possibly be formed at the end of a focused collision sequence (see figure 5a). Assuming that such a defect could perform long-range migration and would appear at the surface as a single extra bright-spot, the model could explain the data. However, it is stressed here that Afman's defect should not require many jumps to recover and was proposed to explain low temperature internal friction relaxation peaks. It is possible that, if such a defect exists, it could tend to trap single SIAs and broaden the observed FIM recovery stage.

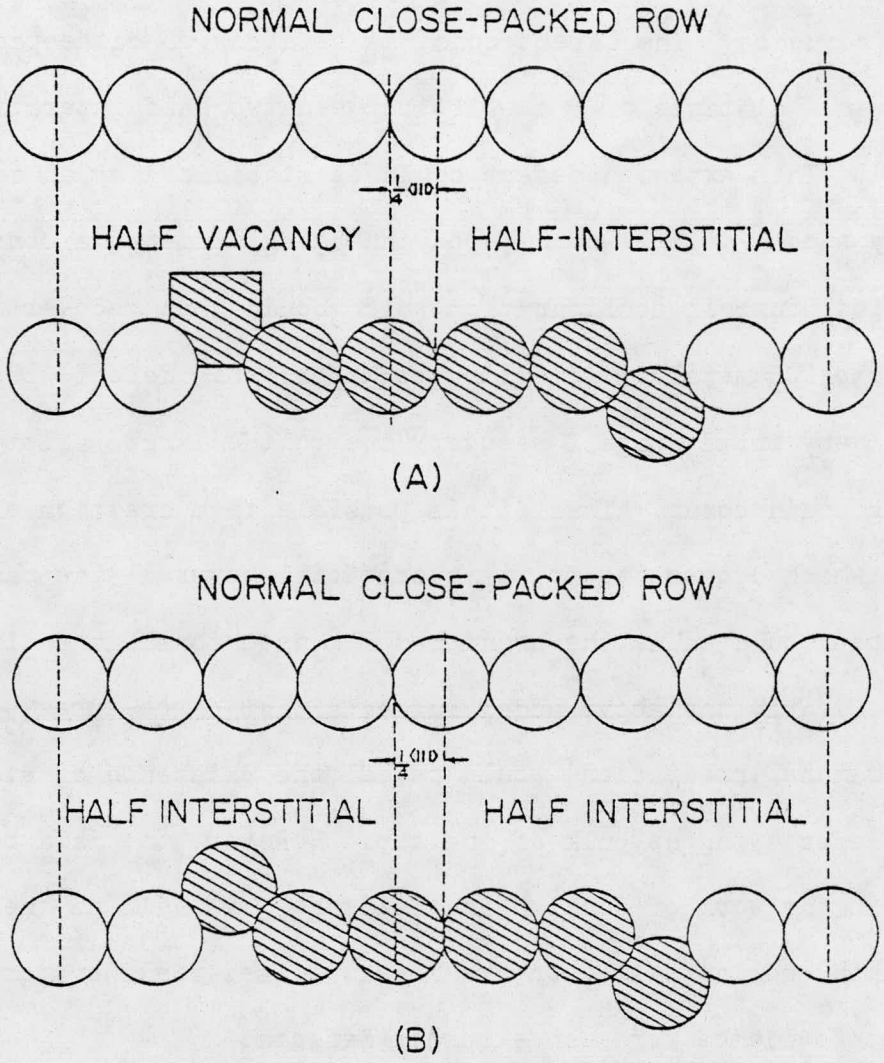

Figure 5a. An extended defect resulting from the shift of a close packed row of atoms over a distance $\frac{1}{4}a\langle 111\rangle$ as proposed by Afman[21]. This shift results in the formation of a half vacancy at the beginning of the row and a half interstitial at the end of the row.

Figure 5b. An extended defect formed from a shift of a row of close packed atoms over a distance $\frac{1}{4}a\langle 111\rangle$ and including an SIA as proposed by Moser[12]. The row begins and ends with a half interstitial.

Moser[12] also proposed a model to explain annealing behavior in BCC metals which offers another extended defect. Defined as a "dissociated crowdion" Moser's defect occurrs at the end of a focused replacement collision sequence. The defect consists of a row of close packed atoms shifted over a distance of $\frac{1}{4}$ a <111> between two half interstitials (see figure 5b). This extended defect could be stabilized by an impurity atom. Supposedly such a defect would, upon annealing, undergo a conversion to the classical dumbell configuration which could then recover in a fashion analogous to FCC metals. According to Moser, this defect would give rise to a very broad stage I recovery due to the large variety of ways detrapping could occur. Thus, it is possible that creation of dissociated crowdions which convert to split-interstitials over a wide range of temperatures could cause the broadened FIM isochronal annealing peak at 38 K. Clearly the above model suggests that a pre-anneal peel (after low temperature irradiation) would reveal the existence of stabilized extended defects in the bulk of the tip. However, the data reported here and in the work of Scanlan and Seidman[6] as well as the work presented in section 2.3.1. on pre-anneal pulsed-field evaporation shows no definite evidence for such extended defects.

2.4. Summary

The results of an FIM study on the 30 keV W^+ ion irradiation of high purity tungsten ($\mathcal{R}$ = 24,000) at 6 K were reported. The pulsed-field evaporation experiments uncovered $1 \cdot 10^{-4}$ at. fr. of immobile SIAs at 20 K. Isochronal anneals following 6 K irradiations generally confirmed the spectra previously obtained by Scanlan, Styris and Seidman[6] and Wilson and Seidman.[7] However, a larger fraction of recovery was observed at

temperatures below those predicted by a diffusion model based on the thermally activated migration of an SIA. The origin of this recovery could only be speculated upon but several possibilities were cited. In previous studies the low temperature recovery was described as a flux of SIAs originally positioned near the surface of the tip. Intrinsic possibilities include: (1) the onset of long-range migration below 30 K followed by SIA-SIA pair migration or dissociation near 38 K; or (2) the existence of another as yet unknown defect which recovers over a broad range of temperatures. At present, it is felt that the very convincing work of Dausinger and Schultz which detected a I_E type substage at $\sim$30 K adds strength to the theory that the major FIM peak at 38 K represents long-range migration below 30 K and SIA-SIA migration or dissociation at 38 K.

With respect to the work of Okuda and Mizubayashi[18] it can be stated that SIAs produced in the bulk at 6 K are still immobile at temperatures as high as 15 K. This is a direct result of the pulsed-field evaporation experiments and is also supported by the isochronal anneals. Furthermore, the recent results of Townsend et al.[26] demonstrated that the onset of long-range migration can not be unambiguously determined by dislocation pinning techniques. It was shown for 10 MeV proton irradiated Cu that dislocation pinning stages were present well below 30 K. However, it had been established that long-range migration does not occur in Cu until above 40 K. Townsend and co-workers observed pinning stages in irradiated tungsten similar to those reported by Okuda et al.[18] but conclude that they are <u>not</u> the result of dislocations pinned by SIAs performing long-range migration.

3. SIA TRAPPING IN TUNGSTEN-RHENIUM ALLOYS

3.1. Review of Literature

It is now highly probable that stage II recovery in tungsten (above $\sim$45 K) involves the formation, rotation, migration or dissociation of defect clusters (SIA or SIA-impurity atom clusters). It has been shown in chapter 2 that the early stage II recovery peaks observed with field-ion microscopy involved the motion of some form of the SIA. This SIA migration could be due to either an intrinsic or extrinsic phenomenon. Wilson and Seidman[22] have demonstrated that both intrinsic and extrinsic mechanisms contribute to the FIM recovery between 45 and 120 K. Their observation that the FIM isochronal annealing spectrum of pure tungsten was insensitive to R values between 15 and $5 \cdot 10^4$ indicated intrinsic behavior. This result was explained by assuming that the distribution of SIAs produced by the 30 keV W^+ ion irradiations in the FIM tip was such that the SIAs only interacted weakly with the impurity atoms (i.e. a small SIA-impurity atom binding energy) and that the SIA-SIA reaction dominated the recovery behavior. Evidence for extrinsic processes occurring during the early part of stage II was also obtained from the carbon doping experiments of Wilson and Seidman[9]. They reported that for pure tungsten doped with $\sim$50-100 appm carbon the long-range migration peak at 38 K was surpressed by approximately 20% while the substage at $\sim$50 K was enhanced. This result suggested that immobile SIA-carbon atom complexes were formed during the long-range migration substage and that the SIAs detrapped at approximately 50 K.

The detrapping of SIAs from impurity atoms during stage II had been studied extensively in FCC metals by electrical resistivity[23]; and internal friction[24]. It has recently been shown by Wei and Seidman[8] that

detrapping of SIAs from impurity atoms can also be studied by the FIM technique. They observed an SIA flux at ∿90 K (stage II) after 30 keV W^+ or Pt^+ ion-irradiation of a series of platinum(gold) FIM specimens. The FIM recovery peaks were fit to a diffusion model for the special case of long-range migration of an SIA in an FIM tip in the presence of impurity atoms. From this fit it was calculated that the dissociation enthalpy (Δh^d_{1i}) was 0.24 eV for substage IIc and by employing 0.05 eV for the value of the motion enthalpy (Δh^m_{1i})[25] it was calculated that the binding enthalpy (Δh^b_{1i}) between a platinum SIA and a gold impurity atom was approximately 0.19 eV for the most tightly bound state. This argument assumed that the dissociation enthalpy is equal to $\Delta h^m_{1i} + \Delta h^b_{1i}$

Wilson and Seidman[9] further reported that upon alloying tungsten with 3 at.% rhenium they observed almost complete suppression of both stages I and II of the FIM isochronal annealing spectrum. They attributed this to a large SIA-Re atom binding enthalpy. It was also reported that no detrapping peak, analogous to that reported by Wei and Seidman, was present below 120 K.

The fact that rhenium atoms trap tungsten SIAs is experimentally important because rhenium is the transmutation product of a beta decay reaction when a tungsten atom captures a thermal neutron ($E_n \leq 1$ MeV)[27]. Since reactor fast neutron fluxes also contain a large thermal neutron component one must consider the effect of introducting small amounts of rhenium on the isochronal recovery behavior of neutron irradiated tungsten. However, to date there have been no low temperature electrical resistivity experiments performed on tungsten doped with small amounts of rhenium to determine the effects of the smaller rhenium atom on stages I and II recovery behavior.

It is the purpose of this chapter to characterize this trapping process

of tungsten SIAs at rhenium atoms by measuring the strength of the binding enthalpy. Wilson and Seidman[9] have established from FIM experiments that SIA trapping occurs below 120 K so that to study the dissociation process it became necessary to extend the isochronal annealing spectrum to higher temperatures until a release peak is observed. The thermodynamic quantity which one obtains from observing a release peak at a given temperature is the dissociation enthalpy which, as mentioned earlier, is taken to be the sum of the binding and motion enthalpies.

Clearly the search for a release peak with field ion microscopy was limited by the temperature range in which the FIM can effectively operate. That is, there existed an upper limit on the annealing temperature to which the search could be extended. It was experimentally determined that the contrast pattern of an SIA, for an isochronal recovery experiment, could be distinguished at temperatures as high as $\sim$390 K. Therefore, before initiating the experiments, the literature was searched for any evidence that might indicate the existence of a release peak within the working temperature range of the FIM.

Unfortunately, the lack of work reported in the literature on the recovery behavior of dilute tungsten(rhenium) alloys made it impossible to determine, with certainty, if a release peak existed below $\sim$390 K. However, since rhenium is produced during thermal neutron irradiation, it should, in principle, have been possible to locate a peak which exhibited the characteristic behavior of a release peak in the recovery spectrum of pure tungsten irradiated to a high dose with thermal neutrons. It is known that the trapping processes are a function of dose, thus the dissociation recovery peak is expected to be dose dependent. That is, since the net effect of increasing the thermal neutron dose is to increase the con-

centration of transmuted rhenium atoms then a release peak would, with reasing dose, become enhanced and shift to higher temperatures. The recovery would become enhanced because more SIAs would become trapped during the long-range migration of the SIAs and therefore more SIAs would be released during dissociation. As the released SIA traveled to a vacancy it would become temporarily retrapped at a number of rhenium atoms. Thus, by increasing the concentration of Re atoms one increases the time required for the SIA to reach a vacancy and hence the peak shifts to a higher temperature.

Probably the single most convincing piece of evidence to be found in the literature of a detrapping peak below 390 K comes from Klabunde et al.'s[16] neutron irradiation work. Polycrystalline tungsten wires were irradiated near 4.2 K to a fast neutron dose of $\sim 10^{20}$ n cm^{-2}. The thermal neutron dose was at least as high as the fast neutron dose. Klabunde et al. reported that between 120 and 300 K the isochronal recovery spectrum exhibited only one peak (at $\sim$280 K) that had the proper dose dependence. That is, upon receiving an increased dose the peak became enhanced and shifted to a higher temperature. The temperature shift was not well pronounced and may have been a result of the lattice weakening effect reported by Keys et al.[29] This weakening effect is reported to be due to the extra electron in rhenium which contributes to the repulsive part of the lattice potential. The net effect would then be to decrease the peak temperature by reducing the migration energy of the SIA and thus negating the effect of increased dose. Regardless of the impurity effects, the existence of a recovery peak which behaved like a detrapping peak within the working range of the FIM was encouraging.

The observation of a release peak around 300 K was later confirmed by

the work of DiCarlo and Townsend[29]; they irradiated tungsten polycrystalline rods (99.8% purity) near 80 K with 13 MeV deuterons. The effects of the irradiation were then observed by internal friction and dynamic Young's modulus measurements taken in the range of 78 to 300 K. An isochronal anneal revealed two thermally-activated relaxation peaks in the internal friction versus temperatures spectra at 115 and 210 K. Both peaks were observed to saturate with deuteron flux. Furthermore, single crystals of high purity tungsten produced neither peak. By comparison with other data DiCarlo and Townsend suggested that the peaks observed during warmup were probably due to one or more of the following defects: (a) a high temperature form of the free interstitial; (b) a free defect complex with more than one intrinsic defect; and (c) an interstitial which had been trapped by other imperfections such as impurities, dislocations, or grain boundaries. The authors were able to eliminate the free intrinsic defect as a possible source of the peaks because of the absence of peak structure in the high purity tungsten spectra. The fact that the concentration of defects producing the peaks saturated with dose, along with the result that the resistivity of the same sample did not saturate with dose eliminates the possibility of an entirely free intrinsic defect complex causing the peak structure. The only remaining explanation is the association of irradiation-induced defects with other imperfections already present in the samples. Annealing to 1500°C or heavy cold-working of the samples left the trap density apparently unchanged. Thus, the authors concluded that impurity trapping of the tungsten SIA was the probable source of the two peaks. Furthermore, it was reported that an anneal to 300 K followed by the measurement of internal friction between 78 and 300K revealed that the peaks had annealed out. That is, by 300 K the impurity-

atom-SIA complex had dissociated. However, the identity of the impurity responsible for the trapping was not determined. Therefore, the work of DiCarlo and Townsend coupled with that of Klabunde et al. strongly indicated that a release peak should be visible within the working temperature range of the field-ion microscope.

Evidence for the existence of a release peak around 200 K was reported by Takamura and co-workers[30]. They measured the recovery of crystalline tungsten wire of a nominal purity ($R \simeq 500$) after fast neutron irradiation at 10 K and various radiation doping treatments. Here, again, there was a very large thermal component to the neutron flux. The radiation doping treatments were performed at $\sim 100^{\circ}C$ and had the net physical effect of introducing immobile vacancies, heterogeneously nucleated interstitial clusters and transmuted rhenium atoms. The isochronal recovery spectra revealed one major peak above 120 K (at $\sim$200 K) after 6 hours irradiation to a fast neutron dose of $\sim 10^{16}$ neutrons cm^{-2}. The behavior of the 200 K peak was characteristic of a long-range migration recovery process. It was enhanced as a result of 64 and 112 hour radiation doping treatments. Furthermore, the peak shifted to lower temperatures as a function of radiation doping. Clearly the addition of transmutation products during the doping process could explain the enhancement effect in terms of a detrapping process, but not the shift to lower temperatures. One expects release peaks to appear at elevated temperatures as a result of the increase in the density of impurity atoms. However, if one takes into account the injection of additional vacancies during radiation doping the two observations become reconcilable with a detrapping model. That is, if the sink density (vacancies) increases faster than the trap density (rhenium impurity atoms) with increasing radiation doping then the distance a released SIA must

travel to recombine with a vacancy decreases. Hence, the enhancement and peak shift of the 200 K peak are consistent with the assignment of de-trapping to the recovery process.

All of the above experiments serve as sufficient evidence to justify an FIM search for the release peak in dilute tungsten(rhenium)alloys. Therefore, a systematic study of tungsten-1 at.% rhenium and tungsten-3 at.% rhenium was initiated, the results of which will be reported in section 3.3.

3.2. Additional Experimental Details

Tungsten alloys of 1 and 3 at.% rhenium were studied. The tungsten-3 at.% rhenium wire was thermocouple wire of diameter 0.1 mm obtained from Omega Engineering, Inc. of Stamford, Conn. The tungsten-1 at.% rhenium was of 0.5 mm diameter polycrystalline wire obtained from Rhenium Alloys, Inc. of Elyria, Ohio. Both alloys were vacuum annealed at 2000°C for 2 hours at a pressure of $1 \cdot 10^{-7}$ torr. The tungsten-1 at.% rhenium wire was electrochemically thinned to 0.1 mm in diameter; a potential of 9 Vdc was applied between the specimen and a stainless steel cathode in an aqueous electrolyte of 1N NaOH. FIM tips were prepared from the annealed wire employing the AC dipping method for both alloys.

An inherent experimental restriction on the FIM technique is that the resolution of the FIM decreases with increasing specimen temperature. This is due to the fact that the image gas ion leaves the tip with a transverse component of velocity determined by the specimen temperature, hence the image size of an atom increases quadratically with increasing temperature.[31] Furthermore, the evaporation field decreases with increasing temperature.[32] Thus, at some elevated temperature the best image field and evaporation field become identical with the end result being that the tip can not be imaged

without field evaporation occurring. Nothing can be done about the first problem (thermal accomodation), but the second one (field evaporation) can be decreased through the proper choice of image gas. The evaporation field of tungsten surface atoms is a fixed function of temperature, thus there is nothing one can do about this parameter. However, the best image field ia a function of many variables one of which can be controlled. The best image field depends strongly on the first ionization potential of the image gas. Therefore, the probability of imaging at elevated temperatures is increased by choosing an image gas with a low ionization potential. Neon is such a gas, relative to helium, and is readily available. It was found that with helium as an imaging gas, SIA contrast was discernable only to about room temperature. With neon as the imaging gas it was possible to maintain atomic resolution up to 400 K.

All irradiations were performed at 18 K in a vacuum $1 \cdot 10^{-9}$ torr with the imaging field off. The isochronal anneals proceeded at a warming rate of approximately 2.5 to 3.0 K min^{-1} in the temperature range of 18 to 410 K. Temperatures above room temperature were achieved by placing a ceramic heater into the cryostat and slowly increasing the heater current. A constant warming rate of 2.5 K min^{-1} was easily maintained.

3.3.2. Continuous Annealing Behavior Between 15 and 400 K

After irradiation at 15 K to a typical dose of $5 \cdot 10^{12}$ W^{+} ion cm^{-2} the tungsten(rhenium)alloys were isochronally annealed at 3 K min^{-1}. A flux of SIAs crossing the tip surface was observed and recorded as a function of temperature. Histograms representing this diffusion process were plotted as the fraction of defects per 5 K interval versus specimen temperature and and are shown in figure 6 and 7. Figure 6 shows the FIM isochronal recovery

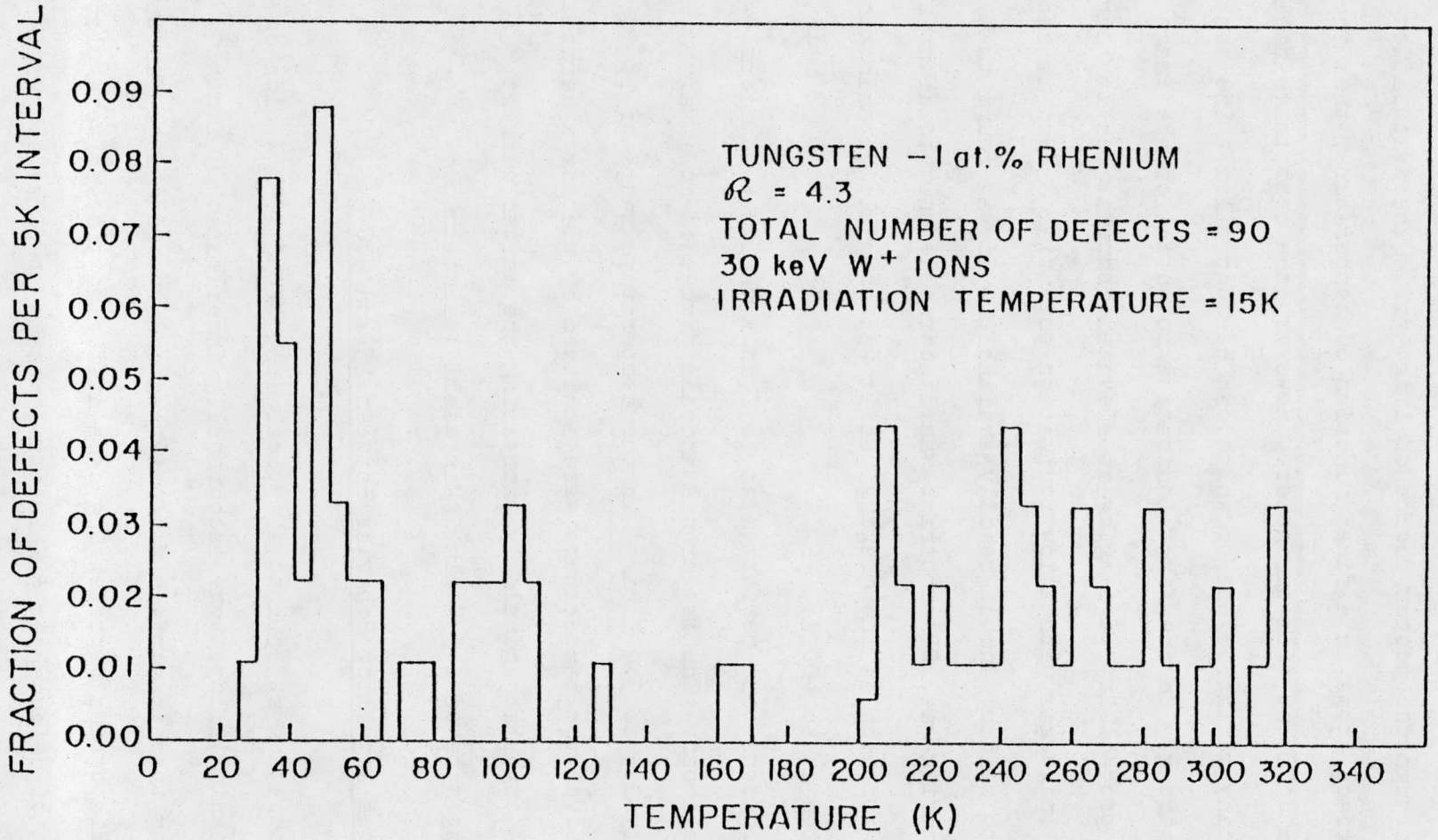

Figure 6. A composite isochronal annealing spectrum for tungsten-1.0 at.% rhenium irradiated at 15 K with 30 keV W^+ ions and annealed to 340 K with a 2.5 k min^{-1} warming rate.

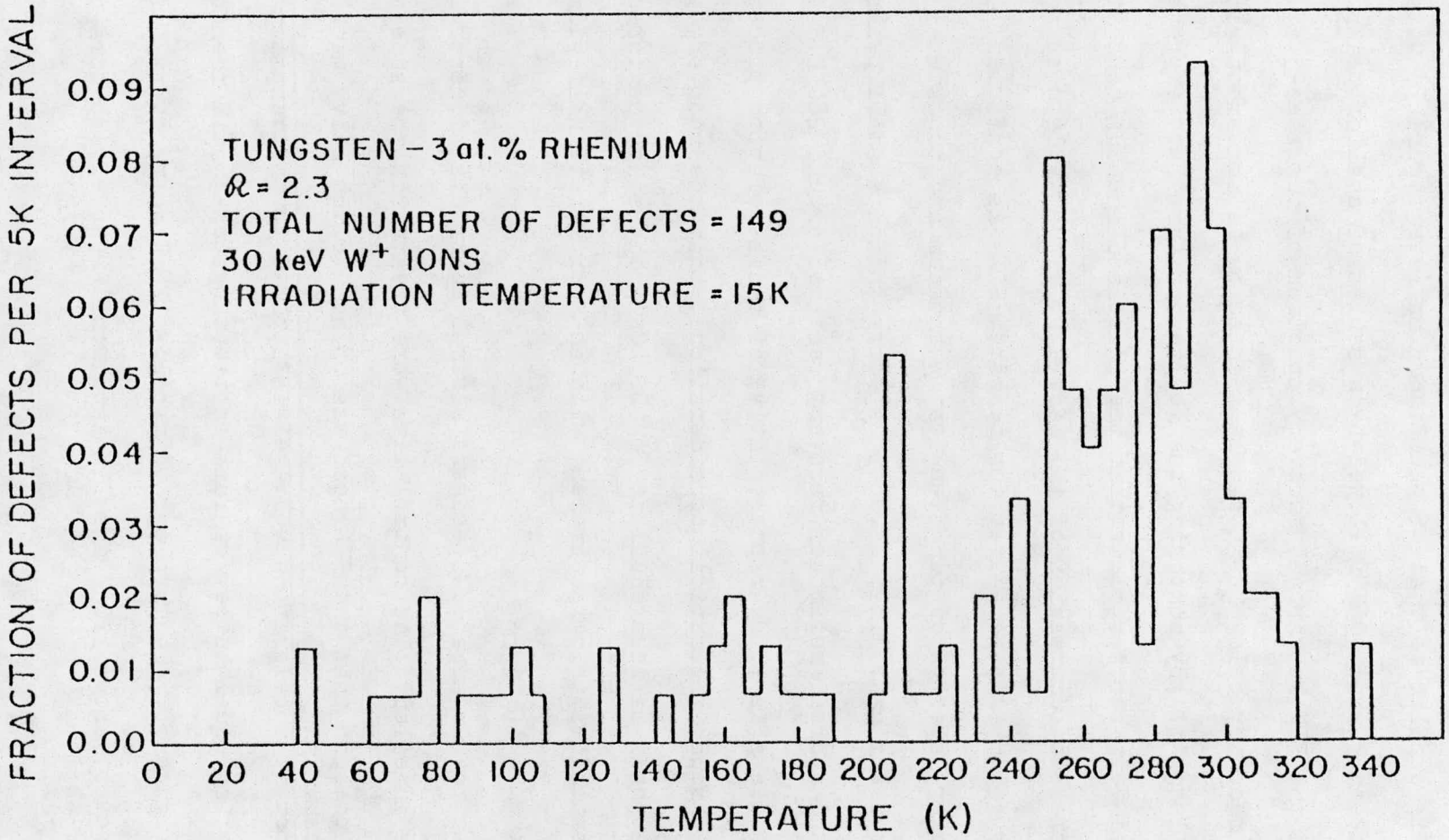

Figure 7. A composite isochronal annealing spectrum for tungsten-3.0 at.% rhenium irradiated at 15 K with 30 keV W^+ ions annealed to 340 K with a 2.5 K min^{-1} warming rate.

spectrum of tungsten-1 at.% rhenium. The low temperature recovery (below 120 K) is similar to that of pure tungsten (see figure 3) with a major peak between 30 and 40 K followed by a series of smaller peaks. Figure 7 shows the FIM isochronal recovery spectrum of tungsten-3 at.% rhenium. The recovery below 120 K can be seen to be in agreement with that reported by Wilson[9]. By comparing the low temperature recovery spectra of figure 6 and 7 it becomes clear that the increased rhenium concentration results in increased surpression of the recovery. Thus, Wilson's[9] conclusion that rhenium acts as a trap for tungsten SIAs is confirmed. Above 120 K the recovery spectra of tungsten-1 at.% rhenium and tungsten-3 at.% rhenium appear identical. That is, both spectra indicate small peaks at 160 K, 210 K and a broad region of recovery centered around 280 K. If one of these three peaks is to be representative of a dissociation process it is necessary, through theoretical consideration*, that the recovery peak have a width at half maximum equal to $T_m/10$. Only the stage centered around 280 K satisfies this requirement with an approximate half-width of 40 K.

Along with the irradiated specimens several unirradiated control specimens were annealed. The control tips were treated in the same manner as irradiated ones in that the FIM head was opened to the heavy metal-ion accelerator, but no accelerating voltage was applied to the tungsten ions. The results for an equal number of runs on the tungsten-3 at.% rhenium are exhibited in figure 8b. It is clear that below 120 K no recovery has occurred. However, above 120 K the FIM isochronal recovery spectra is

---

* The theoretical calculations of Seidman[8], for impurity delayed diffusion in an FIM tip, predicts that for a single thermally activated process an FIM isochronal recovery peak should have a width at half maximum of Tm/10.

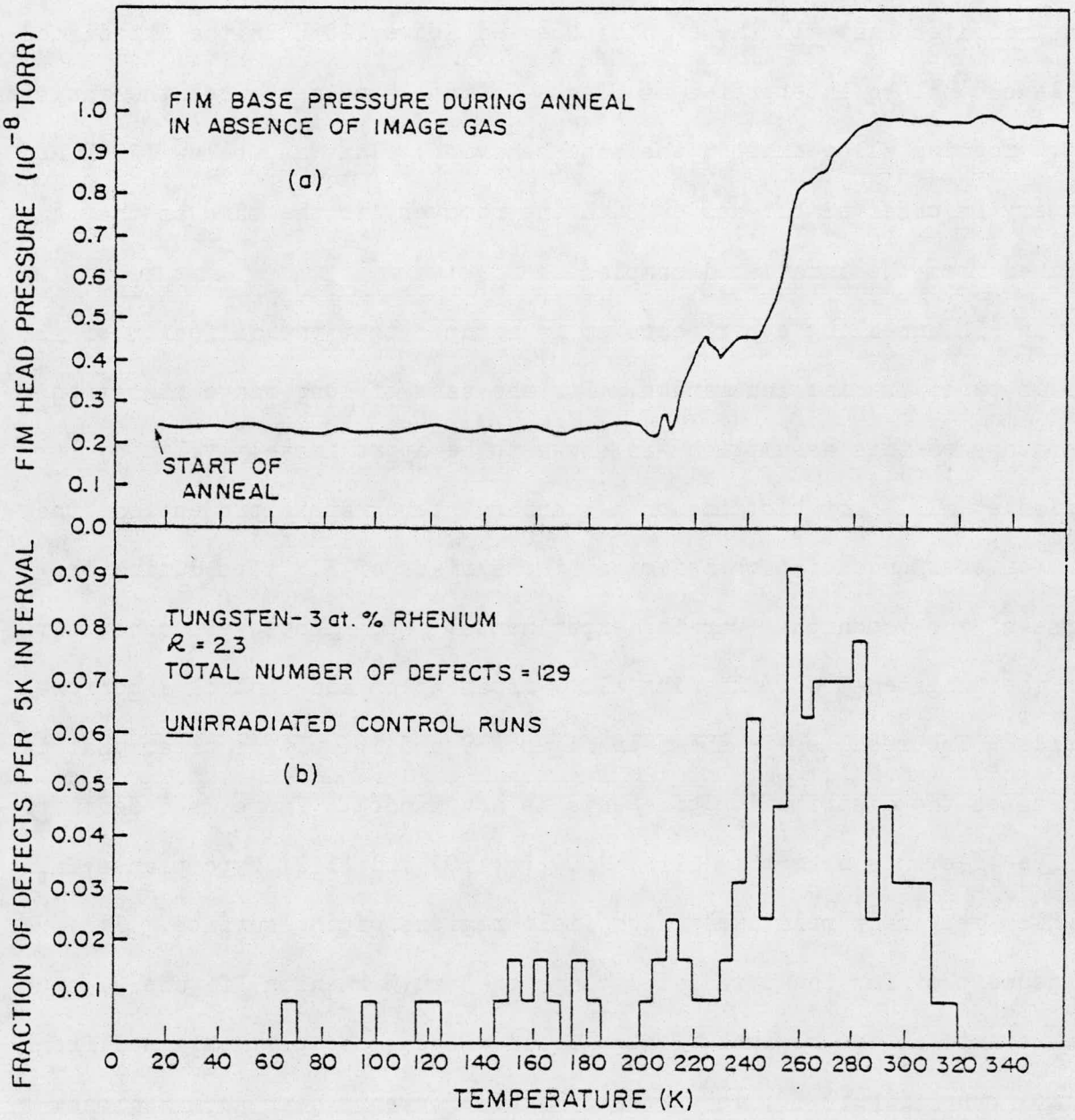

Figure 8a. Base pressure of the FIM during an isochronal anneal plotted as a function of temperature and in the absence of imaging gas.

Figure 8b. A composite isochronal annealing spectrum for unirradiated tungsten-3 at.% rhenium annealed between 15 and 340 K with a 2.5 K min-1 warming rate.

essentially identical to the spectra obtained from the irradiated tips. This indicates that all the events observed above 120 K in the irradiated sample can not be interpreted as SIAs. Control specimens from the tungsten-1 at.% rhenium alloy exhibit the same behavior. That is, below 120 K no recovery is observed but above 120 K the recovery is the same as that obtained from the irradiated samples.

In FIM annealing experiments it is assumed that the diffusion of all SIAs is purely radial and random. For the case of long-range migration in pure tungsten this assumption was shown to be approximately valid by Scanlan et al.[6] by plotting on a standard sterographic projection, the point of emergence of each defect at the surface of FIM tips during the course of the isochronal warming experiments. Such plots were constructed from the tungsten-3 at.% rhenium alloy irradiation and control isochronal anneals. The results are shown in figures 9 and 10. It is clear that in both cases the distribution of events is not random. There is a definite absence of events near the $\{111\}$, $\{100\}$, $\{110\}$ and $\{112\}$ type planes, all of which represent relatively high field regions of the surface. The emergence plot for the irradiated tungsten-3 at.% rhenium, figure 9, shows a few events in the regions of high field whereas the plot obtained from control runs, figure 10, is virtually void of events near such regions. This result is explained by the fact that all of the events recorded in high field regions emerge from the bulk below 120 K and are probably true SIAs.

Origins of the flux of events above 120 K is the topic of the remainder of this section. Certainly, two processes were contributing to this flux; namely surface diffusion and residual gas adsorption. It is known[32] that at elevated temperatures gas contamination on the shank becomes mobile

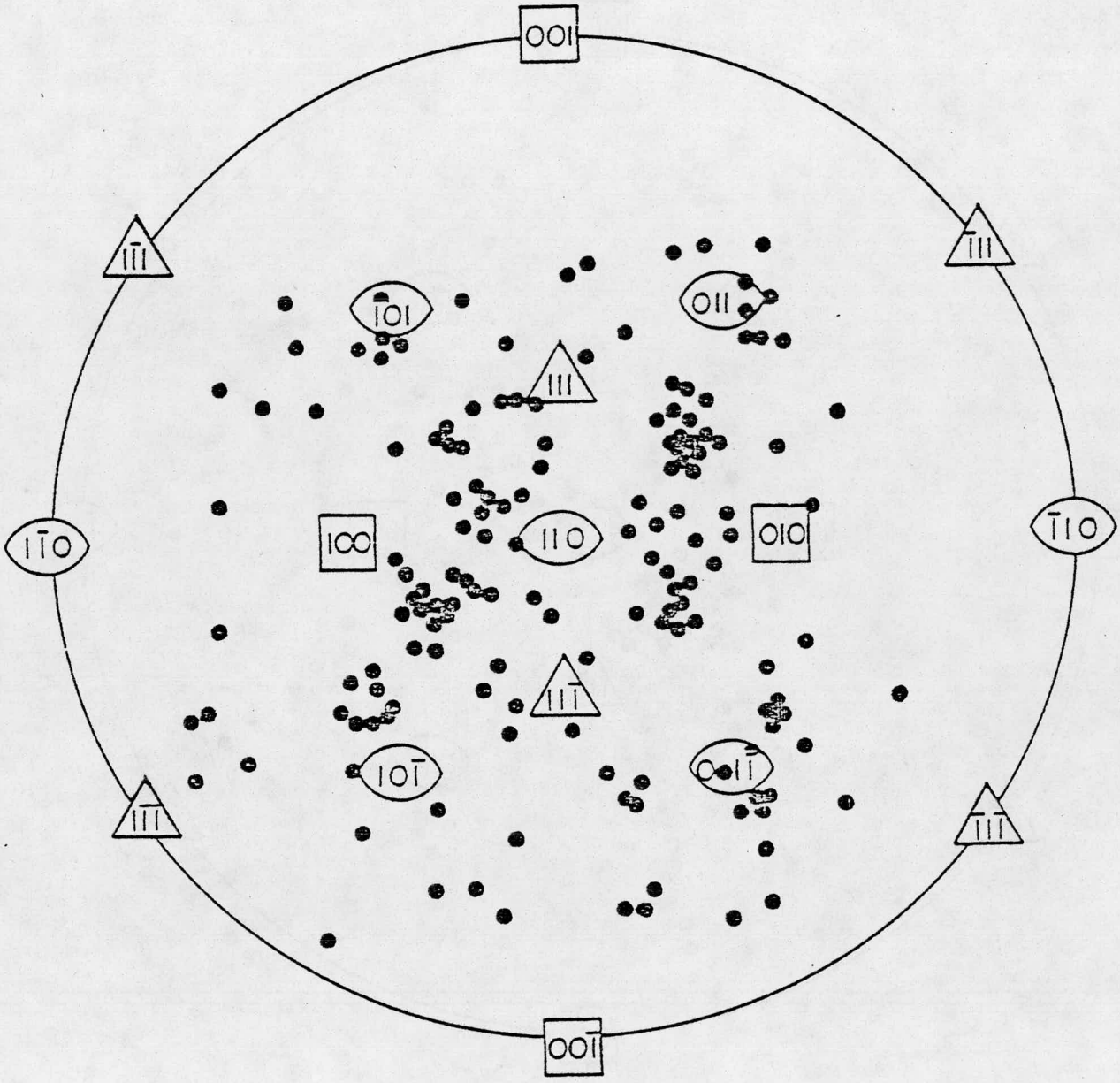

Figure 9. A <110> standard sterographic projection of a cubic crystal. Each black dot marks the point of emergence of an SIA to the surface during a continuous anneal of an FIM specimen. This emergence plot represents a composite of the SIAs observed in the irradiated tungsten-3 at.% rhenium specimens.

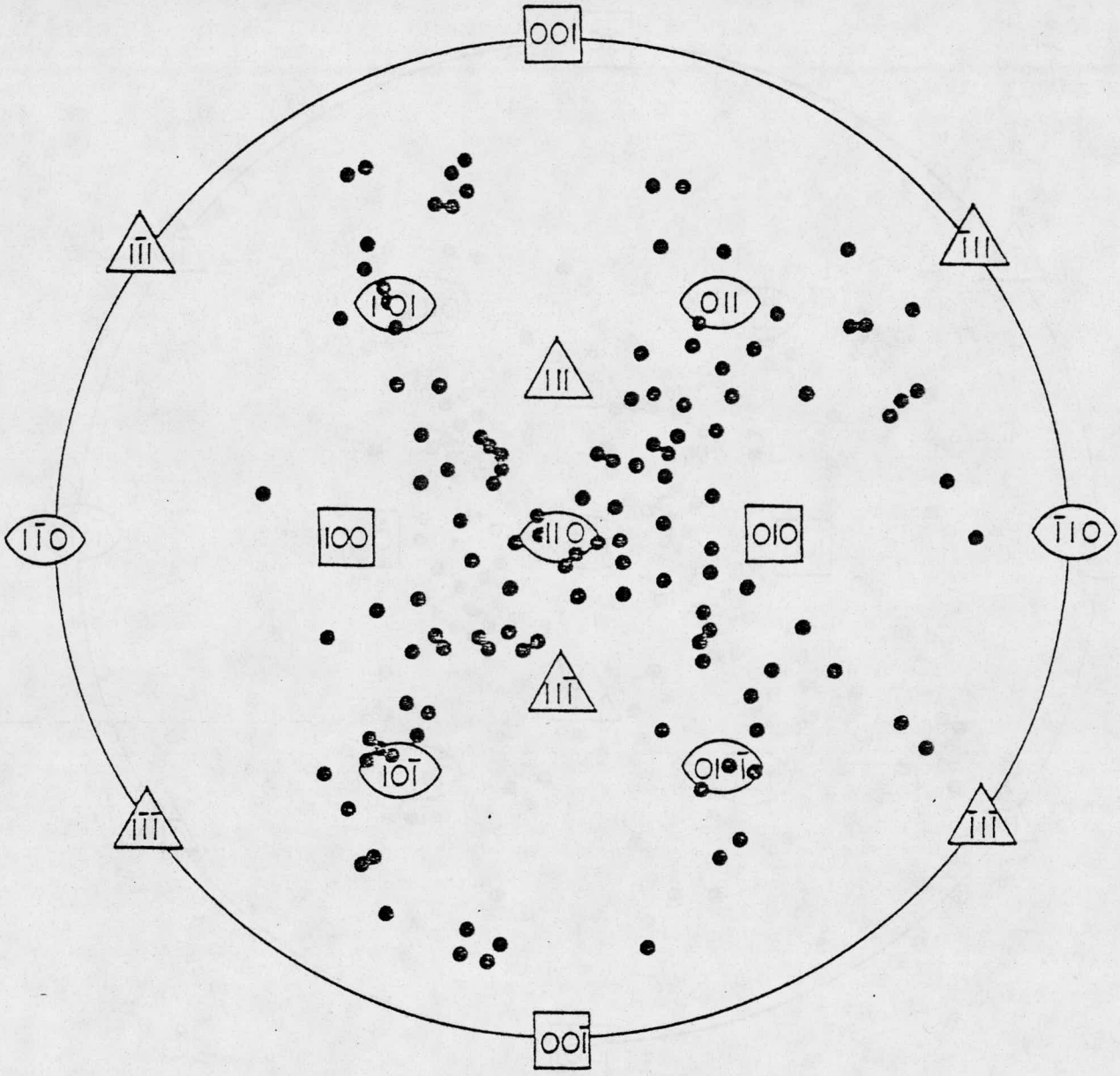

Figure 10. An emergence plot representing a composite of the appearance of extra bright-spots in unirradiated tungsten-3 at.% rhenium during continuous anneal.

enough to diffuse along the surface into the imaged region of the tip. Once on the tip, the diffusing atom could become trapped at a kink site and image as an extra bright-spot. The problem of residual gas adsorption in FIM experiments is compounded by the application of the large electric field to the tip. This field tends to increase the probability of adsorption due to the induced dipole attraction[31].

Since the experimental data suggested that the appearance of the artifact events was temperature dependent a control run was performed which would monitor the system for pressure bursts. The head was dynamically pumped in the absence of an image gas so that small pressure variations could be detected. A control irradiation was performed at 15 K to simulate actual experimental conditions. The head was valved off from the ion pumps and opened to the diffusion pump. An isochronal anneal was then performed at 2.5 K min^{-1} while the pressure was recorded as a function of temperature. The results of the experiment are shown in figure 8a. The head pressure remained constant at $1 \cdot 10^{-9}$ torr until at 200 K where it slowly rose to $8 \cdot 10^{-9}$ torr. Around 230 K the pressure again increased to $1.9 \cdot 10^{-8}$ torr and remained constant for the rest of the anneal. It is clear that the recorded series of pressure bursts constitutes evidence for adsorption of residual gas causing the bright-spot appearance. It was further noted that the spectra of bright-spot events consisted of two major peaks and that the pressure increase was composed of two distinct stages. The first peak of bright-spot events began at 200 K and the second at 240 K. The first stage pressure burst also came near 200 K and the second around 230 K. This correspondence between the FIM base pressure and the artifact contrast effects suggests that the extra bright-spot spectrum could be attributed to residual gas desorbing from the surface of the cryostat

assembly and adsorbing to the slightly cooler tip surface. The character of the residual responsible for the adsorption was not determined.

It was expected that if a release peak existed within the structure above 200 K it would have been clearly visible as a major peak. The fact that the FIM stage I recovery spectra was completely surpressed by trapping suggested that there should have been a large flux of released SIA when kT became large enough. The absence of such a flux could be explained in two ways: (1) the tungsten-rhenium complex has a characteristic dissociation temperature above 400 K; or (2) the SIA releases within the working range of the FIM but becomes trapped in a deeper trap such as a di-rhenium complex. However, as in the case of the tungsten-3 at.% rhenium the 1at.% rhenium isochronal spectra revealed no release peak. Since the concentration of di-rhenium complexes is proportional to the square of the rhenium concentration the 1 at.% rhenium alloy has a factor of nine less di-rhenium complexes. Thus, it is suggested that the SIA rhenium complex has a dissociation energy high enough to remain bound to at least 400 K. On the assumption that $Q = \Delta h^{b}_{1i} + \Delta h^{m}_{1i}$ and taking Δh^{m}_{1i} equal to 0.082 eV[7] the lower limit of the binding enthalpy of rhenium atom to a tungsten SIA was calculated to be $\sim$0.8 eV.

3.3.3. Post Anneal Pulsed-Field Evaporation Experiments

The purpose of the post-anneal pulsed-field evaporation experiments was to directly observe the SIA rhenium complexes. The tungsten-3 at.% rhenium specimen was irradiated to a dose of $5.9 \cdot 10^{12}$ at 15 K followed by an isochronal anneal to 120°C. This allowed the stage I SIA to migrate to the surface or to a rhenium atom. The tip was then cooled down to 15 K and a

pulsed-field evaporation experiment performed. A total of $1.1 \cdot 10^5$ atoms were counted and 11 complex contrast patterns were observed, thus implying a concentration of $\sim 1.0 \cdot 10^{-4}$ at.fr. These complex contrast patterns were unlike any of those observed in our earlier studies. They were different from both the stage I SIA and solute atom contrast patterns. Furthermore, they differed from what would be expected for a single SIA based on a theoretical contrast model worked out by Seidman and Lie.[14]

One of the eleven complex contrast patterns is shown in figure 11 as an evaporation sequence. It was possible to compare the similarities of the above complex contrast patterns with those observed by Wilson and Seidman[9] in the 2.35 MeV electron irradiated tungsten. Pulsed-field evaporation experiments were performed on commercially pure tungsten irradiated to a dose of $1 \cdot 10^{20}$ electron cm^{-2} at ~ 430 K. Wilson and Seidman reported unusual contrast patterns which were similar to those observed in this study. It was concluded that the complex contrast patterns must have been caused by a cluster of point defects made up of either: (1) vacancies; (2) SIAs; or (3) SIAs trapped at impurity atoms. Vacancy clustering was ruled out because this point defect is immobile at the irradiation temperature. Thus, it was suggested that the complexes were either SIA clusters or, more probably, SIA-impurity atom clusters. The fact that the complex contrast patterns were present only in the <u>irradiated</u> tungsten-rhenium alloys plus the striking similarity to those reported by Wilson and Seidman implies that the SIA rhenium complexes were observed.

It should also be noted here that the observation of stable SIA-rhenium complexes up to 120°C can be used to interpret other stage III FIM experiments. In particular, the work of Attardo et al.[33] should be re-

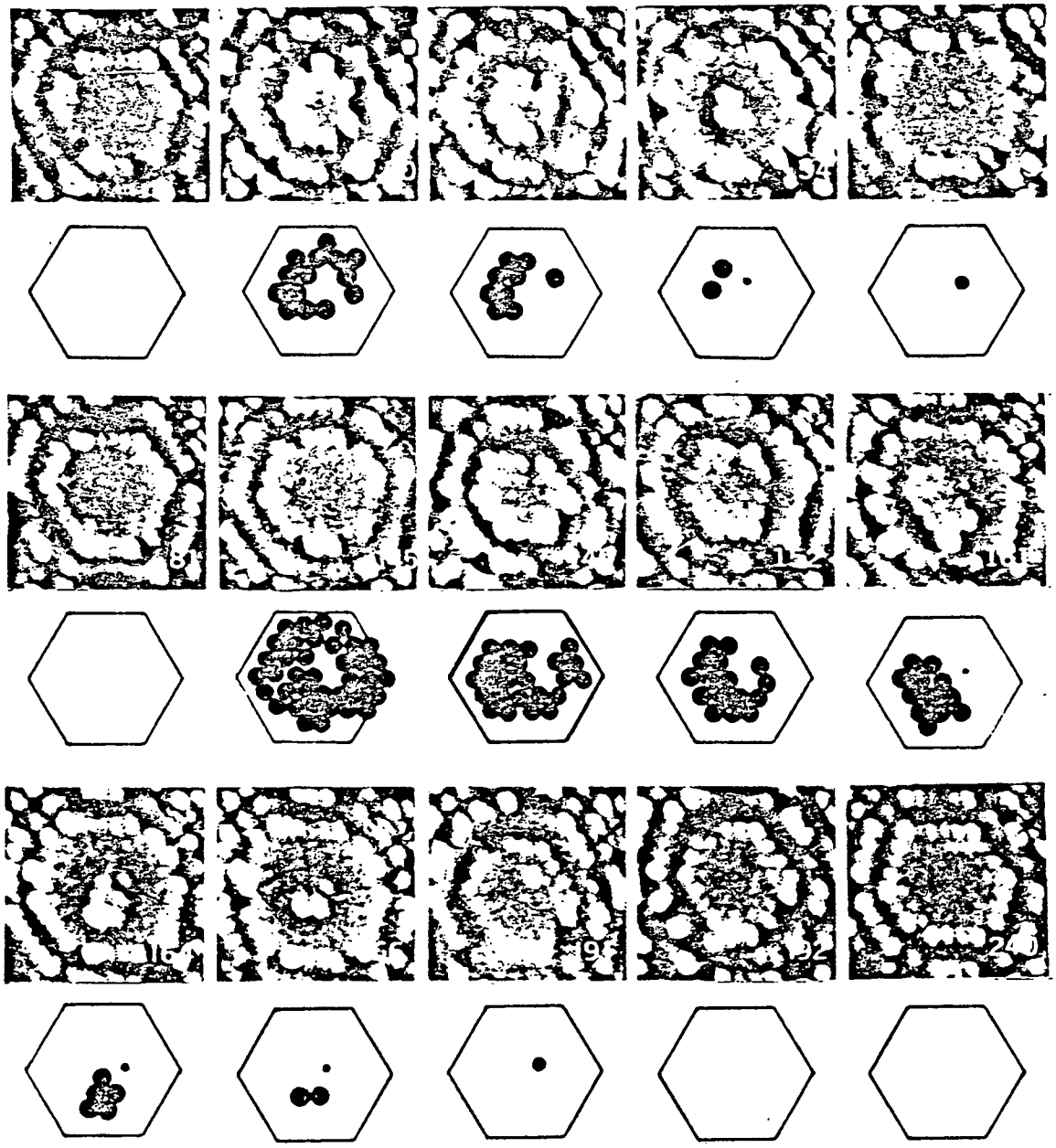

Figure 11. A series of 15 micrographs showing a complex contrast pattern on the (111) plane of tungsten-3 at.% rhenium. Frame 1 shows a full plane which will be called layer 1. Frame 50 shows a plane just beneath layer 1 in which 2 vacant sites are present. Frame 54 shows the first extra bright-spot which lingered until frame 81. The next plane, layer 3, was perfect. Layer 4 contained two vacancies in frames 145 through 160. Frame 161 shows the appearance of the second extra bright-spot. The extra bright-spot lingers until frame 191 when it evaporates. The next two layers were perfect.

analyzed. They irradiated high purity ($R \simeq 4 \cdot 10^4$) tungsten specimens at 100°C to a dose of $5 \cdot 10^{19}$ fast neutrons cm^{-2} and a thermal neutron dose which was at least twice the fast neutron value. Their FIM investigation detected single vacancies, clusters of vacancies and single extra bright-spots. The extra bright-spots were anisotropic and the long axis of some of the extra bright-spots was approximately parallel to a 110 type direction. As a result of annealing the specimens for 1 hour at 400 C (in stage III) the concentration of extra bright-spots decreased from 10^{-3} to 10^{-5} at.fr. and simultaneously the concentration of vacancies decreased from $2 \cdot 10^{-3}$ to $1.3 \cdot 10^{-3}$ at.fr. They interpreted their observations in terms of the migration of SIAs to vacancies in stage III. The reason it is felt that the work of Attardo et al. relates to the data presented in this chapter centers around the fact that their thermal neutron dose ($\sim 10^{20}$ cm^{-2}) results in the transmutation of tungsten to rhenium. It has been shown experimentally that a dose of 10^{20} thermal neutrons cm^{-2} yields a rhenium concentration of 10^{-3} at.fr.[27] which corresponds closely to their extra bright-spot concentration. It has been shown in this chapter that SIAs are trapped by rhenium atoms at the irradiation temperature employed by Attardo et al. Furthermore, it has been experimentally shown that: (1) the contrast patterns produced by single rhenium atoms[9] are different from the extra bright-spot pattern presented by Attardo et al.; and (2) the contrast pattern of a SIA-Re complex resembles their extra bright-spot pattern. Thus, it is highly likely that the extra bright-spots observed by Attardo et al. were SIA-Re clusters. Hence, the observed decrease in the concentration of extra bright-spots is interpretable in terms of vacancy migration to a SIA-rhenium complex. The rhenium atom remaining after the annihilation of the SIA produces a subtle contrast pattern[9] which requires, in many

cases, careful pulsed-field evaporation experiments to detects and not simply the controlled field-evaporation technique.

3.4. Summary

A systematic suppression of the FIM isochronal recovery below 120 K in irradiated tungsten(rhenium) alloys (1 and 3 at.%) reaffirmed the existence of trapping of tungsten SIAs at Re atoms. Above 120 K a series of broad recovery peaks were found in both tungsten(rhenium) alloys irradiated with 30 keV W^+ ions. However, identical recovery structure was observed in the unirradiated tungsten(rhenium) control experiments. Therefore, no unambiguous released peaks could be identical from the FIM isochronal annealing spectra.

Furthermore, it was suggested that the presence of complex contrast-patterns randomly distributed throughout the bulk of an irradiated tungsten-3 at.% rhenium sample after annealing to 390 K probably represented the direct observation of SIA rhenium complexes. It was therefore concluded that rhenium atoms trap tungsten SIAs in W(Re) alloys with sufficient strength to remain bound up to at least 390 K.

4. FIM STUDY OF STAGE I RECOVERY OF IRRADIATED MOLYBDENUM

4.1. Review of Literature

The stage I annealing behavior of irradiated molybdenum has been the subject of several experimental studies in the past 15 years. Unlike tungsten the recovery spectrum obtained for molybdenum is remarkably reproducible in most labs.[23] However, besides the temperatures of the major substages little else concerning the recovery of molybdenum has been agreed upon. In particular, the substage associated with long-range migration of the molybdenum SIA (analogous to substage I_E of FCC metals) has yet to be conclusively identified. In fact, controversy still persists on whether or not the SIA performs long-range migration at all in stage I. This fact characterizes the fundamental question of the analogy between low temperature recovery substages in BCC and FCC metals. Therefore, it would be extremely useful to know if long-range migration occurs in molybdenum.

In an FIM isochronal annealing experiment only those recovery processes involving long-range migration can be observed. It is therefore the aim of this work to identify the temperature at which such processes occur, if at all, in heavy-ion irradiated molybdenum. Additional insight should also be gained into the FCC analogy problem, that is, if no long-range migration is found in stage I an analogy between FCC and BCC recovery would be highly unlikely. Alternatively, if a well behaved long-range migration stage is observed the FCC-BCC analogy may be useful.

A review of the most recent work reported for stage I reveals widely ranging temperature assignments for the onset of long-range migration in

molybdenum. Okuda's[34] internal friction results indicate a long-range migration of SIAs at temperatures as low as 30 K while the resistivity measurements of Horak and Blewitt[35] suggest migration temperatures as high as 70 K. A brief review of the work done to experimentally identify the temperature associated with long-range migration in irradiated molybdenum will be presented in this section.

The recent work of Okuda and Mizubayashi[34] on the internal friction of molybdenum after fast neutron irradiation at 4.2 K revealed evidence of a long-range migration stage centered around 30 K. Oriented single crystal, high purity (ℓ = 4000) molybdenum plates were irradiated near liquid helium temperature and subsequently annealed to 300 K. During the anneal the internal friction and dynamic modulus were measured by the electrostatic flexural vibration method. Two relaxation peaks were observed in the internal friction spectrum at 11 and 39 K. It was noted that the 11 K peak annealed out after warming to 30 K and the 39 K peak recovered near 45 K. Furthermore, two pronounced increases in the dynamic modulus (or pinning stages) were present at about 30 and 42 K. Dislocation density and dose dependence experiments indicated that there were two types of interstitials contributing to the pinning at both 28 and 42 K. The authors suggested that the 11 K relaxation peak was due to close pair rotation and the 39 K peak was associated with detrapping of SIAs. Therefore the two pinning substages could be attributed to long-range migration of the free SIA at 30 K and that of the detrapped SIA at 42 K.

Another series of investigations was recently carried out by Moser and co-workers [36, 37, 38] on the internal friction and electrical resistivity recovery of 3 MeV electron and fast neutron irradiated molybdenum wires. Polycrystalline wires with ℓ = 100 were fast neutron irradiated

(E > 1 MeV) at 28 K to a dose of $5 \cdot 10^{17}$ neutron cm^{-2} or electron irradiated (E = 3 MeV) at 20 K to a dose of 10^{18} electron cm^{-2}. After fast neutron irradiation the internal friction spectrum revealed relaxation peaks at 31 and 40 K. It was found that both peaks recovered simultaneously after warming to 43 K. Moser et al. proposed the "frozen free-split" mechanism described by Nowick[39] to explain both peaks. The corresponding defect, probably a <110> free interstitial (in agreement with the recent Huang diffuse scattering results of Erhart[40]), would have two modes of relaxation each with a unique relaxation time. This single defect could therefore give rise to both internal friction peaks. The electrical resistivity results were similar to those obtained by Lucasson et al.[41] after electron irradiation, and by Takamura et al.[42] after neutron irradiation. Thermodynamic consideration of the recovery spectra led Moser and co-workers to assign long-range migration to a substage at 42 K, thus forcing agreement with their internal friction results.

The experiments of Hanada et al.[43] offer yet another interpretation of the annealing stages of low-temperature irradiated molybdenum. Wire specimens ranging in purity from $\mathcal{R}$ = 20 to 520 were fast neutron irradiated at 10 K to varying doses and subsequently annealed. The recovery spectrum, which has recently been confirmed by Vajda and Biget[44], contained several large peaks below 100 K. In an effort to identify the peak associated with long-range migration the effects of radiation doping and impurity content on the low temperature recovery stages were examined. Radiation doping introduces Frenkel pairs at high temperatures (below stage III) and results in a defect distribution consisting of several isolated vacancies and a few interstitial clusters. It was found that such an initial defect concentration enhanced the amount of recovery in stages I

and II. This enhancement tended to saturate with dose and was found to almost entirely anneal out by 400°C. Furthermore, the amount of enhancement was found to be proportional to the doped vacancy concentration and not the SIA cluster concentration. This behavior could only be explained on the basis of a model wherein SIAs sampled much of the lattice before annihilating at vacancy sites. Therefore, it was concluded by Hanada et al. that SIAs were performing long-range migration in both stages I and II. Observation of the effects of increasing impurity content on low temperature recovery stages has been used to determine the defect involved with that stage in many FCC metals. Close-pair recovery stages would be unaffected by impurity content whereas long-range migration peaks tend to become surpressed due to trapping processes. Hanada et al. observed a steady suppressed of the recovery stage centered at 60 K with decreasing R values (increasing impurity concentration). This was the only recovery stage that exhibited systematic behavior and was considered to be analogous to the impurity dependence of peak I_E in Cu which was interpreted as long-range migration of SIAs. It was noted by the authors that their results were in agreement with the work of Lomer et al.[45] who observed an internal friction dislocation pinning stage between 50 and 70 K in high purity molybdenum due to the long-range migration of the SIA.

The most recent, and probably the most convincing, study of long-range migration in molybdenum was published by Coltman et al.[46] The purpose of their experiment was to record the effects of initial dose and radiation doping upon the low temperature recovery stages of molybdenum. Wire specimens of R = 1900 were either fission or thermal neutron irradiated at 4.9 K to a wide range of doses. The basic recovery spectrum bears a close resemblance to the recovery pattern of the FCC metals.

Close-pair substages appear at 14, 23 and 27 K and a major stage at 40 K appears to represent correlated recovery. It was anticipated that if the FCC model was valid for molybdenum then the substage analogous to I_E (long-range migration) would be characteristically influenced by increasing dose and radiation doping. As a result of increasing the dose two effects were observed: (1) the subpeak centered at 47 K moved to a lower temperature such that it became lost in the 40 K peak; (2) the amount of recovery observed for the 40 and 47 K subpeaks was enhanced. The behavior of the 47 K substage was identical to that of its substage I_E FCC counterpart and the coupled relationship between the 40 and 47 K stages was also similar to that seen between the I_D and I_E stages in FCC metals. Furthermore, the results of the radiation doping experiments showed that enhanced recovery of the doped specimens began near 42 K and proceeded in a manner consistent with that for FCC metals. Coltman et al. therefore concluded that the recovery in stage I of molybdenum could be identified with stage I of the FCC metals and that correlated and uncorrelated long-range migration were represented by substages centered at 40 and 47 K respectively. It should be noted here that the assignment of 47 K to the onset of long-range migration has recently been confirmed by the electron damage rate experiments of Antesberger et al.[47].

Finally, it is for the sake of completeness that the work of Afman[48] be mentioned in this review. Afman attempted to model the annealing behavior of electron irradiated molybdenum wires by observing the influence of varied incident electron energy on the recovery spectrum. Molybdenum wires of $\mathcal{R} = 900$ were irradiated with 1.85 MeV electrons at 4.2 K. The resulting annealing spectrum consisted of major recovery substages centered at 20, 25 and 40 K. Upon lowering the energy from 1.85 to 1.05 MeV, the

recovery between 30 and 45 K was enhanced and the substage at 25 K was markedly suppressed. It was expected that if the irradiation energy was lowered the substages which correspond to defects with a higher threshold energy of formation should be suppressed. Therefore, substages involving long-range migration should be suppressed. Through kinetic arguments Afman reported that none of the suppressed peaks could represent uncorrelated long-range migration. To explain the absence of such a peak Afman developed a two defect model comprised of the typical Frenkel pair and an as yet undefined defect. Close-pair recovery could therefore be assigned to the substage at 20 K and correlated recombination to the peak at 25 K. The recovery peak at 40 K was then ascribed to the second defect. Phenomenalogically, Afman suggested that SIAs which escape correlated recombination at 25 K are trapped by either impurity atoms or by the second defect. This point was experimentally substantiated by the measurement of higher damage production rates at 40 K than at 60 K. Afman therefore concludes that since SIAs cannot make enough jumps to perform uncorrelated recombination without becoming trapped the attempt to identify a I_E type stage in irradiated molybdenum must be considered meaningless.

It should be noted here that there are two points made by Afman which have been criticized. First, the use of kinetic theories, and therefore curve fitting, to draw conclusions is questionable. Secondly, it has been suggested that incident energy effects in electron studies are difficult to see because only small populations of free defects are produced due to the low energy recoils associated with electron irradiation.

It is clear from the above review of recent literature, there still remains a tremendous amount of controversy over not only the assignment of

a temperature to long-range migration in molybdenum, but also over the general correlation between BCC recovery and FCC recovery. Table 2 serves as a summary of the work cited here and can be seen to illustrate the wide range of experimental results reported for the onset of long-range migration.

4.2. Additional Experimental Details

Commercially pure molybdenum in the form of 20 cm long rods with initial diameters of 1.5 mm were obtained from Materials Research Corporation (MRC). The preparation of high purity, single crystal molybdenum from these rods was carried out employing the procedure developed by Capp et al.[49] Electron beam zone refining of the rods was carried out under a vacuum of 10^{-6}torr. Prior to melting, specimens were outgassed by passing a hot zone ($\sim 2000^{\circ}C$) rapidly up the rod. Single crystals were grown by passing a molten zone with a maximum length of $\sim$1 cm along the rod. Each crystal was given 2 zone passes at a speed of $\sim$0.5 cm min^{-1}. After zone-refining, the crystals were subjected to a two-stage annealing treatment; first in an oxygen partial pressure of $6 \cdot 10^{-5}$torr at $1600^{\circ}C$ for 4 hours to reduce the carbon level, and second under a vacuum of 10^{-6}torr at $1800^{\circ}C$ to remove oxygen. The decarburisation and deoxidation treatments resulted in molybdenum resistivity ratios of 5700.

The single crystals of molybdenum were then thinned to $\sim$0.5 mm diameter by electropolishing at 20 Vdc in a solution of 3 parts H_2SO_4 to 7 parts (by volume) ethyl alcohol. The rod was then sectioned into 1.5 cm lengths by the dc drop-off technique. During the drop-off each section was further thinned to a diameter of 0.1 mm. The sections were then polished into FIM tips by the dc drop-off technique (see section 1.3.1.) in a solution of 1

TABLE 1

Summary of Work Done Previously on Molybdenum Stage I Recovery

AUTHORS	REFERENCE NO.	TECHNIQUE	RESISTIVITY RATIO ($\rho_{300K}/\rho_{4.2K}$)	IRRADIATING SPECIES	LONG-RANGE MIGRATION TEMP
Okuda et al.	34	Internal Friction	4000	Fast Neutrons	30 K
Moser et al.	36 37 38	Internal Friction Electrical Resistivity	100	Fast Neutrons 2 MeV Electrons	42 K
Coltman et al.	46	Electrical Resistivity	1900	Thermal Neutrons	47 K
Antesberger et al.	47	Electrical Resistivity	1000	3 MeV Electrons	47 K
Hanada et al.	43	Electrical Resistivity	500	Fast Neutrons	60 K
Afman	48	Electrical Resistivity	900	2 MeV Electrons	None

part H_2SO_4 to 9 parts ethyl alcohol.

4.3. Results

4.3.1. Continuous Annealing Behavior Between 10 and 120 K

After irradiation at 10 K to a typical dose of $5 \cdot 10^{12}$ ion cm^{-2} (Mo^+ ions) the high-purity molybdenum specimens were isochronally annealed at a warming rate of less than 2 K min^{-1}. The surface of the tip was monitored by continuously photographing at a rate of 1 frame per 3 seconds or approximately every tenth of a degree Kelvin. Figure 12 shows the surface of a Mo tip as viewed by the ciné camera. The contrast effect associated with the arrival of an SIA to the surface of molybdenum was found to be identical to that for tungsten; that is, zero contrast to full contrast within one frame. Examples of the appearance of extra bright-spots is shown in figure 13 for several different locations on the surface.

The results of recording the arrival of SIAs (or extra bright-spots) as a function of temperature are shown for 2 PZR molybdenum irradiated at 10 K in figure 14. This figure represents a composite of 4 runs. The important features of this annealing spectrum are a major peak centered at 32 K, a minor peak at 45 K and a characteristic long tail extending to 120 K. It should also be noted that very few events were recorded below 25 K. The major peak at 32 K in the annealing spectrum of molybdenum most certainly represents the onset of long-range migration and hence the termination, by definition, of stage I recovery. Therefore, the next peak, at 45 K, must be considered a stage II phenonenon and may represent an impurity detrapping process or di-SIA migration or dissociation.

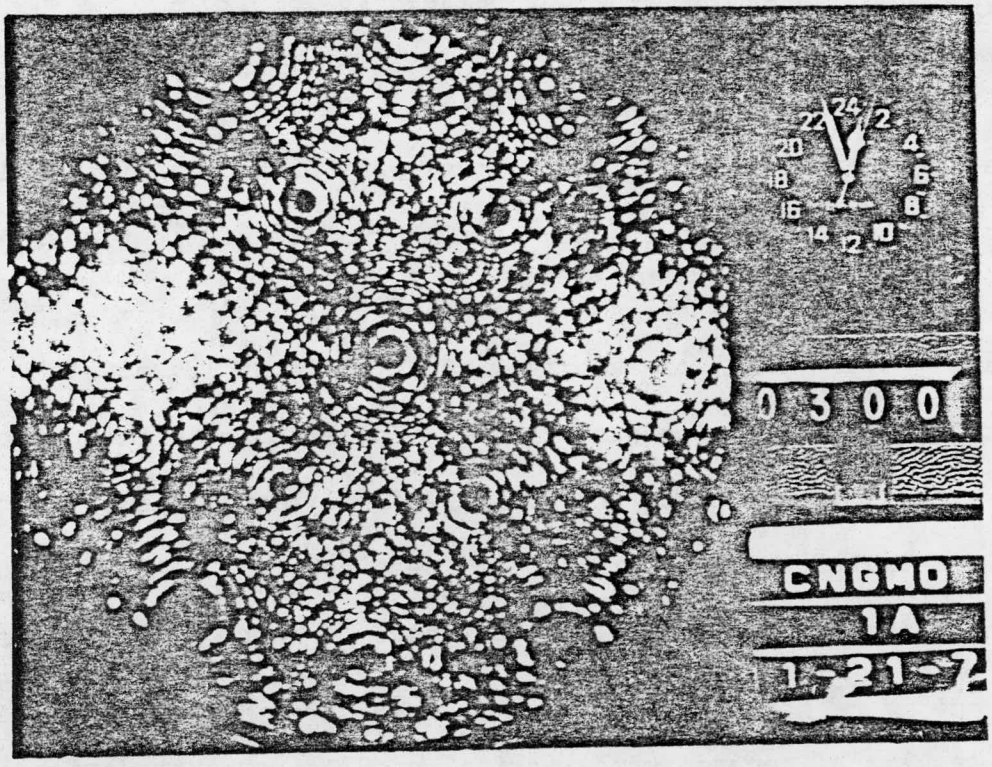

Figure 12. A FIM micrograph of a molybdenum specimen at 30 K during a continuous anneal showing several extra bright-spots on the surface. The data chamber can be seen on the right side of the micrograph.

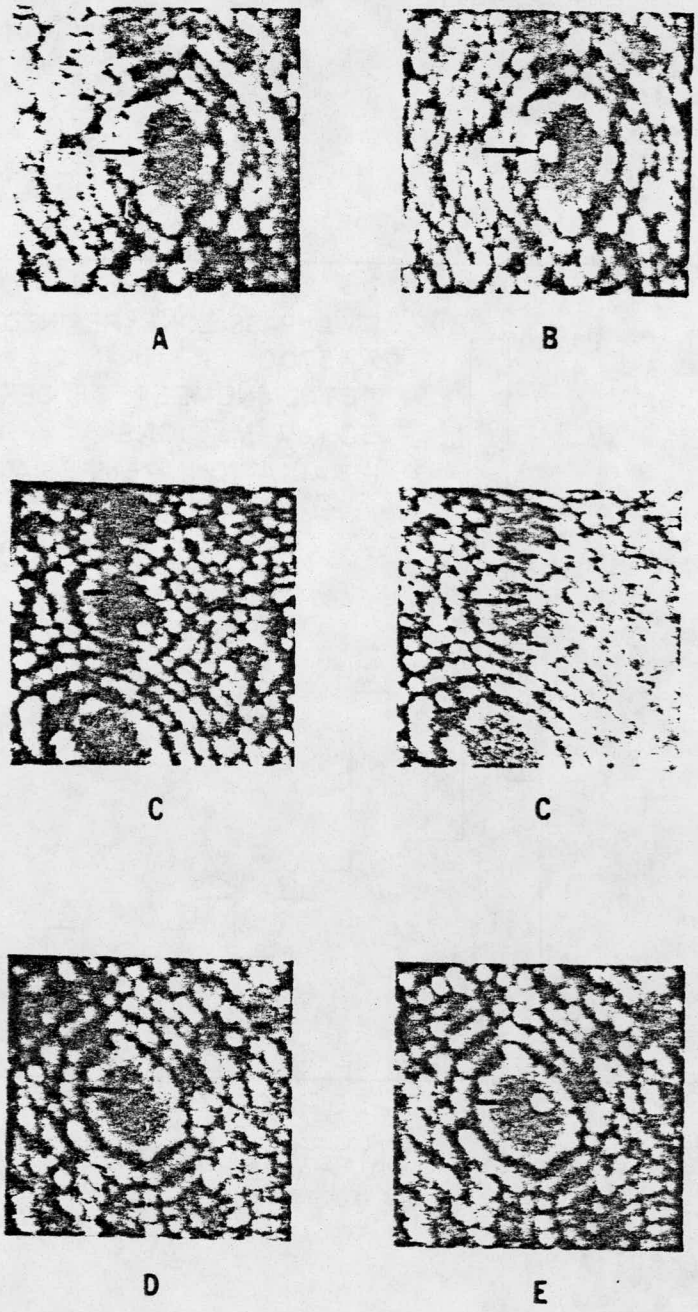

Figure 13. (A,B) The appearance of a single spot SIA contrast pattern at 35 K on the (100) plane of molybdenum imaged at 8 kV.

(C,D) The appearance of a single spot SIA contrast pattern at 37 K on the (334) plane of molybdenum imaged at 8 kV.

(E,F) The appearance of a single spot SIA contrast pattern at 39 K on the (112) plane of molybdenum imaged at 8 kV.

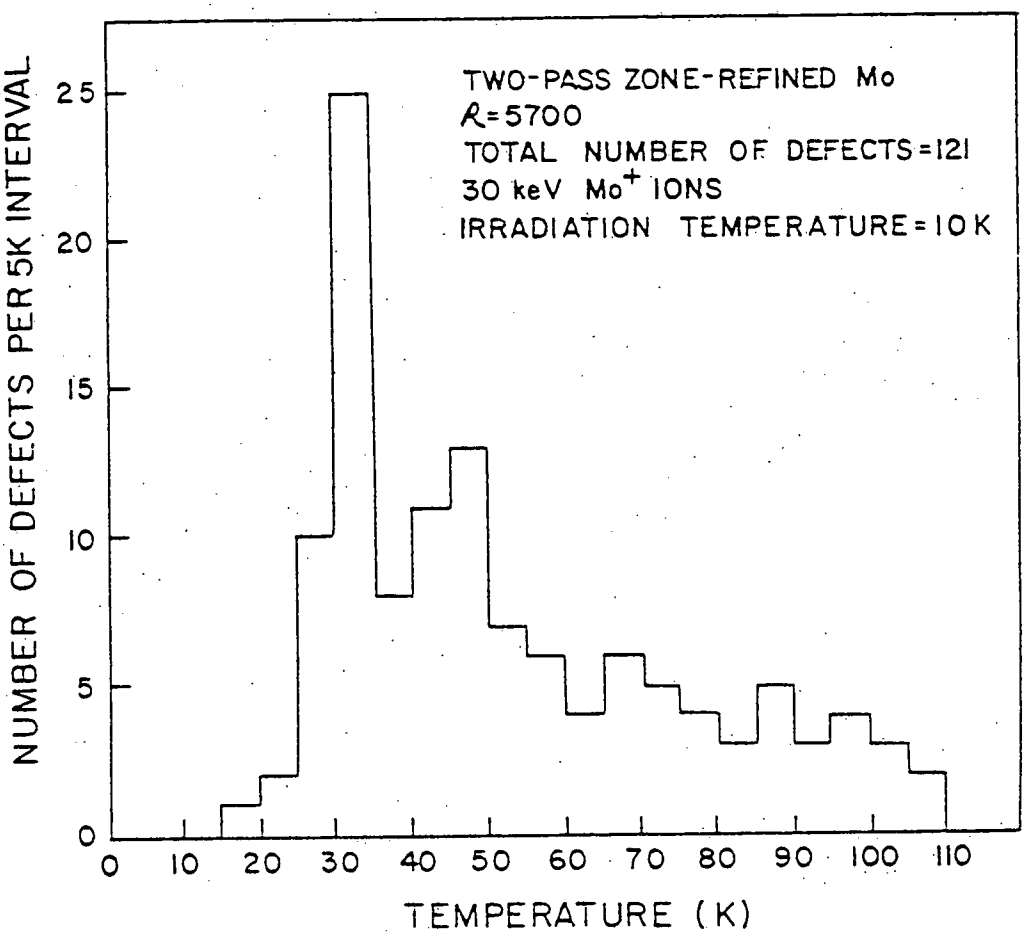

Figure 14. A composite isochronal annealing spectrum for two-pass zone-refined molybdenum irradiated at 10 K with 30 keV Mo^+ ions and annealed to 120 K with a 2 K min^{-1} warming rate.

As noted in chapters 2 and 3, the hypothesis that the flux of extra bright-spots to the surface represents a random diffusion process can be tested with an emergence plot. Such a plot is presented in figure 15. Superimposed on this plot is a set of concentric circles, representing equal areas on a hemisperical tip. The number of extra bright-spots found in each area element is plotted as a function of θ and ϕ (both from the <110> fiber axis) and shown in figure 16. Obviously, the observed distributions (representing SIA flux) were not perfectly isotropic. However, this deviation from ideal behavior was small to assume that radial diffusion was valid as a first approximation.

In order to analyze the experimental peak width, the data from the 32 K peak was replotted as the number of defects observed per 2.5 K temperature interval. Data was obtained from four irradiations on the same specimen so that effects due to inhomogeneities in the specimen material were minimized. That is, the possible broadening due to the superposition of many runs on tips of different radii and slightly different composition was eliminated. The 32 K peak overlaped the 45 K, therefore, the end of the long-range migration peak could not unambiguously be determined. Hence, the termination of the 32 K peak was set at 35 K. The events observed below 35 K for the four isochronal annealing experiments are shown in figure 17. Superimposed on the experimental data is the calculated curve for the flux of a single thermally activated SIA diffusing in a spherical FIM tip. The curve was positioned such that: (1) the maximum occurred at 32.5 K; and (2) the areas under the calculated and experimental curves were equal to each other. The superposition of the calculated curve yielded a

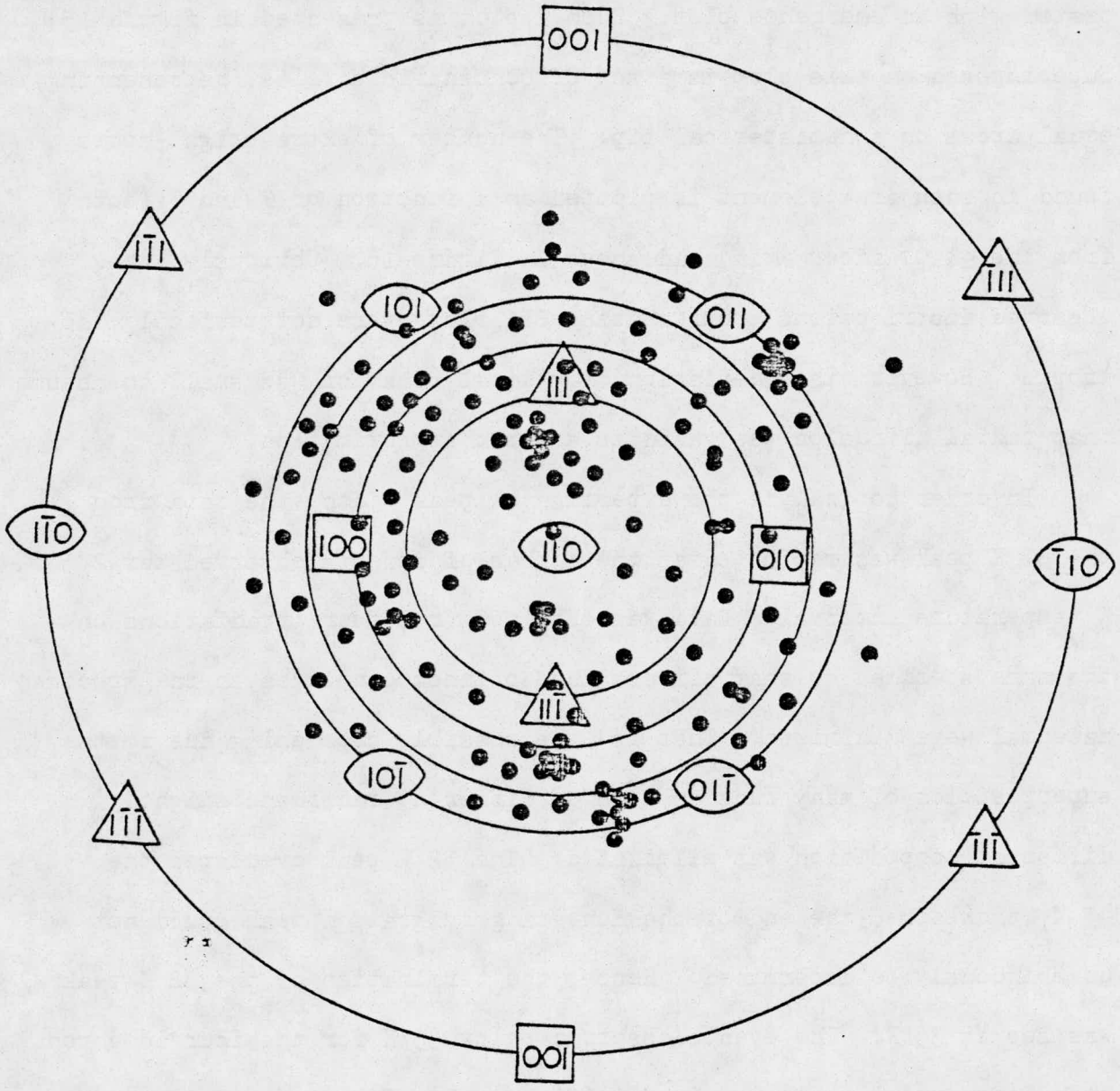

Figure 15. A <110> standard stereographic projection of a cubic crystal. Each black dot represents the point of emergence of a molybdenum SIA, during a continuous anneal, on the surface of FIM specimens with <110> fiber axes. The circles represent regions of equal area on the surface.

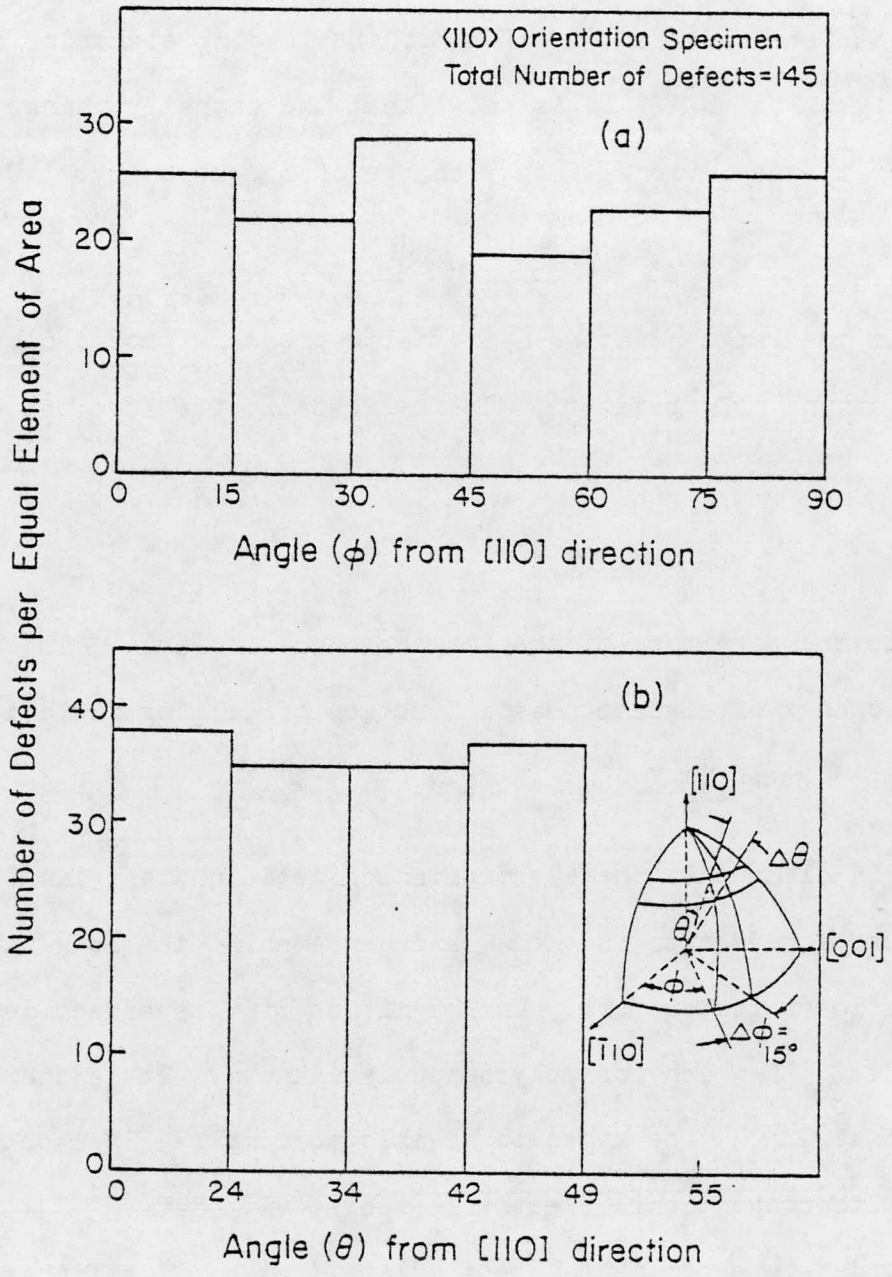

Figure 16a. The number of defects per equal element of area as measured in the ϕ direction.

Figure 16b. The θ dependence of the distribution of the distribution of defects on the surface of the specimen. This distribution was plotted from the data shown in figure 15.

$\Delta h^m_{1i} = 0.08$ eV for the dimensionless parameter Γ equal to 10^{16}.

The question most often associated with FIM isochronal annealing experiments is: What was the effect of the imaging electric field on the diffusivity of the SIA? It is known that the enthalpy change of migration is related to the internal energy change of migration by:

$$\Delta h^m_{1i} = \Delta u^m_{1i} + p\Delta v^m_{1i} \quad , \tag{4.1}$$

where p is the large negative hydrostatic pressure produced on the specimen during FIM operation. The hydrostatic pressure can be written as:

$$p = -E^2 \cdot (8\pi)^{-1} \tag{4.2}$$

Where E is the magnitude of the imaging electric field. Therefore, the enthalpy change of migration as a function of imaging field is given by:

$$\Delta h^m_{1i} = \Delta u^m_{1i} - E^2 \cdot (8\pi)^{-1} \Delta v^m_{1i} \, . \tag{4.3}$$

Thus, it is clear that the electrostatic field inherent in FIM experiments could cause a reduction in Δh^m_{1i} and hence shift the long-range migration peak to a lower temperature. The magnitude of this effect depends on the value of Δv^m_{1i} which for molybdenum is unknown. It is therefore important that Δv^m_{1i} be known to be able to compare FIM isochronal annealing spectra with conventional electrical resistivity data.

In order to experimentally calculate Δv^m_{1i} it suffices to show that the SIA is mobile at temperatures slightly above the observed long-range migration peak. To this end 2 PZR molybdenum specimens of $\mathcal{R} = 5700$ were irradiated <u>in situ</u> with 30 keV Mo^+ ions at 40 K in the absence of the imaging electric field and imaging gas. The specimens were then quickly cooled to 10 K, the imaging gas reintroduced and electric field reapplied.

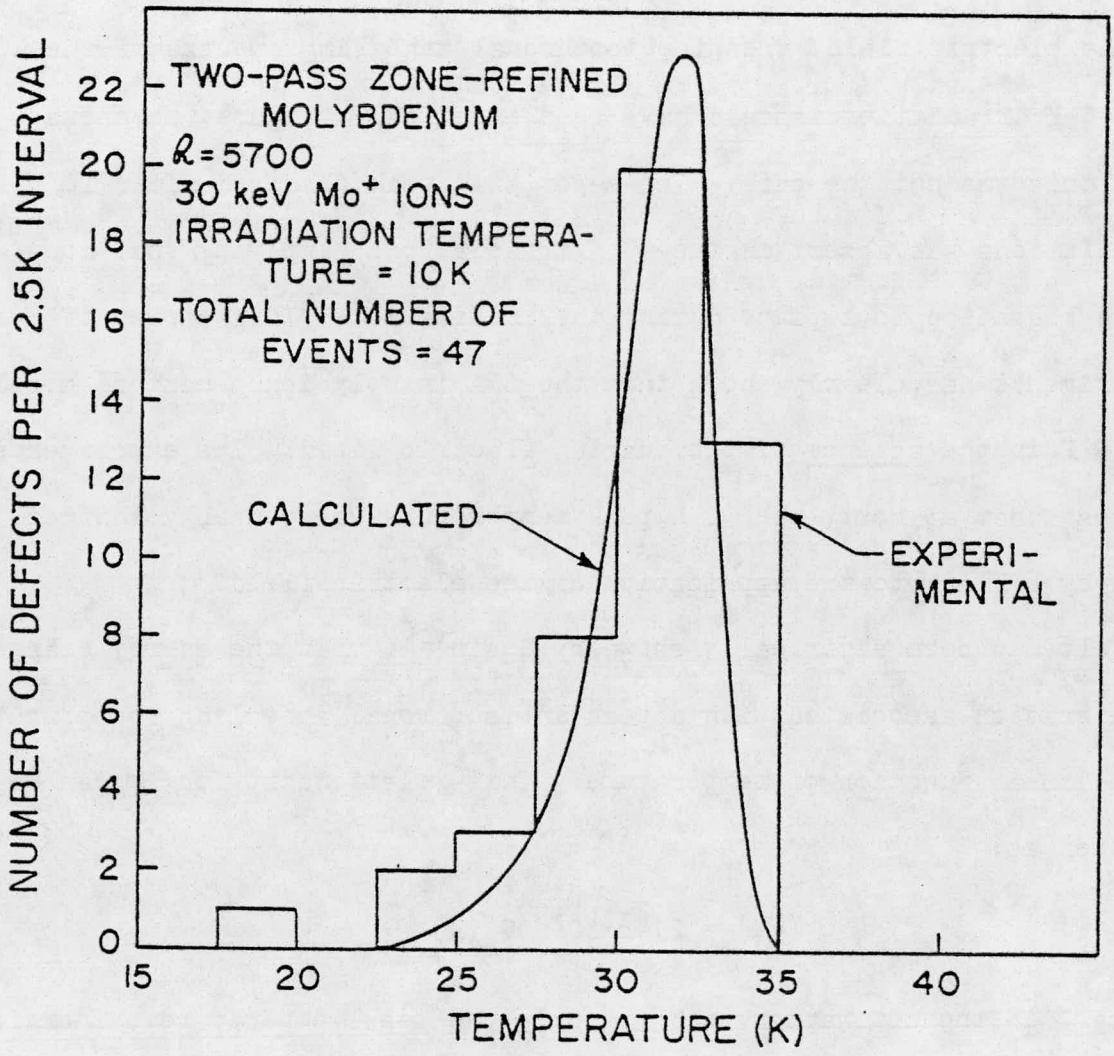

Figure 17. A composite isochronal annealing spectrum for two-pass zone-refined molybdenum plotted with 2.5 K temperature intervals. Only the SIA events below 35 K are included in this histogram. A calculated isochronal annealing spectrum for a single thermally activated defect is superimposed on the experimental results.

The remainder of the procedure was identical to the 10 K irradiations. The results of 3 such irradiations are shown in figure 18b. Figure 18a is a composite also of 3 irradiations performed at 10 K plotted as the number of defects (or events) observed per 5 K temperature interval. If the long-range migration of the SIA occurred above 40 K in the absence of the electric field, then the isochronal annealing spectra of the 10 K and 40 K irradiations should have been identical. Figure 18b shows that this was not the case. The major 32 K peak observed after 10 K irradiations was absent in the 40 K irradiations, implying that long-range migration took place during the irradiation. This series of experiments has clearly shown that the SIA in molybdenum must be mobile at 40 K in the absence of the imaging electric field. The experiments suggest that at most, the 32 K peak temperature was possibly shifted down by 8 K due to the application of the electric field.

It has been empirically shown by Sosin[50] that the energy change of migration associated with a peak in isochronal annealing spectrum is a linear function of temperature. This relationship for Mo can be written as:

$$Q\ (eV) = 2.46 \cdot 10^{-3}\ T_m(K) \qquad (4.4)$$

where Q is the activation energy and T_m the peak temperature. Therefore, to obtain an upper limit, a shift of 8 K in peak temperature corresponds to an energy change of ~ 0.02 eV produced by the $p\Delta v_{1i}^m$ term. The pressure can be calculated from $E^2(8\pi)^{-1}$ assuming an imaging field of 3.50 V_A^{-1}[32] Substitution of this pressure into equation 4.3 gives an upper limit to the volume change of migration equal to:

$$\Delta v_{1i}^m \leq 0.04 \Omega_a \qquad (4.5)$$

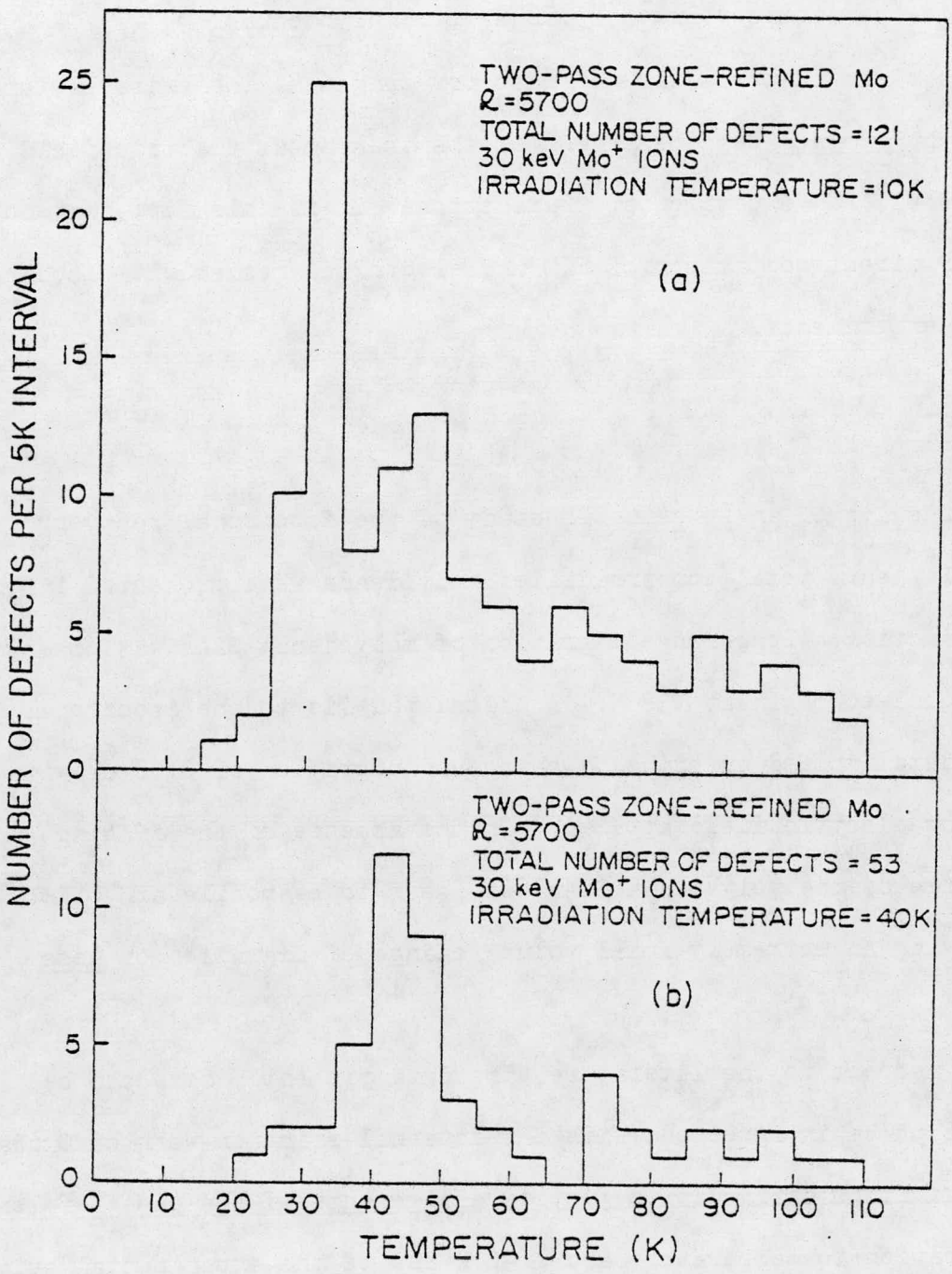

Figure 18a. A composite isochronal annealing spectrum for two-pass zone-refined molybdenum irradiated at 10 K with 30 keV Mo^+ ions and annealed to 120 K with a 2 K min^{-1} warming rate.

Figure 18b. A composite annealing spectrum for two-pass zone-refined molybdenum irradiated at 40 K with 30 keV Mo^+ ions and cooled to 10 K in the absence of an electric field. The specimens were then annealed from 10 K to 120 K with a 2 K min^{-1} warming rate.

where Ω_a is the atomic volume (15.92 A^3 for molybdenum).

It is clear that, as was the case for tungsten, the extremely small value of Δv^m_{1i} negates the effect of the tremendous electric field present in all FIM experiments. Furthermore, it is this fact that now allows for direct comparison of FIM and electrical resistivity isochronal annealing experiments.

4.4. Summary

The results of an in situ FIM study of the isochronal recovery behavior in heavy metal ion irradiated molybdenum were presented in the previous section. Long-range migration of molybdenum SIAs was observed and was found to begin at $\sim$32 K. A calculated fit to the isochronal recovery data implied an enthalpy change of migration of 0.08 eV with the imaging electric field applied. In the absence of the imaging electric field, the molybdenum SIAs were seen to be mobile at 40 K thus implying an extremely small volume change of migration of less than $0.04\,\Omega_a$.

With respect to the literature, the data presented here can be considered to be in agreement with the internal friction work of Okuda et al.[34] It is difficult to justify assignments of the onset of long-range migration to temperature above 40 K due to the experimental evidence presented here that the molybdenum SIA is already mobile at 40 K.

The results here are also in good agreement with the electron irradiation damage rate experiments of Maury et al.[51] Their analysis of the displacement energy and orientation dependence of the recovery substages below 50 K in electron irradiated molybdenum

suggested that the 33 K stage could be attributed to long-range migration of SIAs formed along <111> displacement chains.

References

1. M.W. Thompson, Defects and Radiation Damage in Metals (Cambridge, University Press, Cambridge, 1969) p.1.

2. A. Seeger, in Fundamental Aspects of Radiation Damage in Metals, edited by M.T. Robinson and F.W. Young (National Technical Information Service, Springfield, VA 1975) pp. 493-517.

3. W. Schilling, in Fundamental Aspects of Radiation Damage in Metals, edited by M.T. Robinson and F.W. Young (National Technical Information Service, Springfield, VA 1975) pp. 470-492.

4. M.K. Sinha and E.W. Muller, J. Appl. Phys. 35, 1256(1964)

5. J.M. Galligan, in Vacancies and Interstitials in Metals, edited by A.Seeger, D. Schumacher, W. Schilling and J. Diehl (North-Holland, Amsterdam, 1970) pp. 575-588.

6. R.M. Scanlan, D.L. Styris and D.N. Seidman, Phil. Mag. 23, 1439(1971).

7. K.L. Wilson and D.N. Seidman, Rad. Eff. 27, 67 (1975).

8. C-Y. Wei and D.N. Seidman, Cornell University Materials Science Center Report No. 2392 (1975).

9. K.L. Wilson, PhD. Thesis, Cornell University (1975).

10. K.L. Wilson and D.N. Seidman, in Defects and Defect Clusters in BCC Metals and Their Alloys, edited by R.J. Arsenalt (National Bureau of Standards, Gaitherburg, Maryland, 1973) pp. 216-239.

11. H. Schultz, in Defects in Refractory Metals, edited by R. DeBatist, J. Nihoul and L. Stals (Mol, Belgium, 1971) pp. 383-394.

12. P. Moser, in Defects in Refractory Metals, edited by R. DeBatist, J. Nihoul and L. Stals (Mol, Belgium, 1971) pp. 59-74.

13. D.N. Seidman and R.M. Scanlan, Phil. Mag. 23, 1429 (1971).

14. D.N. Seidman and K.H. Lie, Acta Met. 20, 1045 (1972).

15. W. Kunz, K. Faber, R. Lachenmann and H. Schultz, in Defects in Refractory Metals, edited by R. DeBatist, J. Nihoul and L. Stals (Mol, Belgium, 1971) pp. 7-12.

16. C.E. Klabunde, R.R. Coltman Jr., A.L. Southern and J.K. Redman, Bull. Amer. Phys. Soc. 16, 319 (1971).

17. F. Dausinger, H. Schultz, K. Boning and G. Vogel, Tagongstortrag Physikertagung in Freudenstadt, April (1974).

18. S. Okuda and H. Mizubayashi, Phys. Rev. Lett. 34, 815 (1975).

19. F. Dausinger and H. Schultz. Phys. Rev. Lett. 10, 57(1975).

20. J.R. Beeler in Defects and Defect Clusters in BCC Metals and Their Alloys, edited by R.J. Arsenalt (National Bureau of Standards, Gaitherburg, Maryland, 1973) pp. 582-602.

21. H.B. Afman, in Defects in Refractory Metals, edited by R. DeBatist, J. Nihoul and L. Stals (Mol, Belgium, 1971) pp. 19-22.

22. K.L. Wilson and D.N. Seidman, Cornell University Materials Science Center Report No. 2347 (1974).

23. J. Nihoul, in Vacancies and Interstitials in Metals, edited by A. Seeger, D. Schumacher, W. Schilling and J. Diehl (North-Hollard, Amsterdam, 1970) pp. 839-888.

24. J.A. DiCarlo and J.R. Townsend, Acta Met. 14, 1715 (1966).

25. P. Petroff and D.N. Seidman, Acta Met. 21, 323 (1973).

26. J.R. Townsend, Phys. Rev. B 122, 41 (1976).

27. L.K. Keys and J. Moteff, Phys. Rev. 176, 851 (1968).

28. L.K. Keys and J. Moteff, J. Nuclear Mat. 33, 337 (1969).

29. J.A. DiCarlo and J.R. Townsend, Acta Met. 14, 1715 (1966).

30. S. Takamura, R. Hanada, S. Okuda and H. Kimura, J. Phys. Soc. Japan 30, 1091 (1971).

31. E.W. Muller and T.T. Tsang, in Field Ion Microscopy, (American Elsevier Publishing Company, New York, 1969) p.40.

32. D.G. Brandon, in Field Ion Microscopy, edited by J.J. Hren and S. Ranganathan (Plenium Press, New York, 1968) p.66.

33. M.J. Attardo, J.M. Galligan and J.G.Y. Choy, Phys. Rev. Lett. 19, 73 (1967).

34. S. Okuda and H. Mizubayashi, Crystal Lattice Defects 4, 75 (1973).

35. J.A. Horak and T.H. Blewitt, J. Nuc. Mat. 49, 161 (1974).

36. R. Pichon, E.A. Bisogni and P. Moser, in Defects in Refractory Metals, edited by R. DeBatist, J. Nihoul and L. Stals (Mol, Belgium, 1971) p. 39.

37. V. Hivert, R. Pichon and P. Moser, J. Phys. Chem. Solids, 31, 1843 (1970).

38. P. Moser, J. Verdone, W. Chambron, V.Hivert and R. Pichon, J. Phys. F 3, 363 (1973).

39. A.S. Nowick, Scripta Met. 7, 289 (1973).

40. P. Erhart, in Fundamental Aspects of Radiation Damage in Metals, edited by M.T. Robinson and F.W. Young (National Technical Information Service, Springfield, VA 1975) pp. 302-308.

41. P. Lucasson and R.M. Wilson, Phys. Rev. 127, 485 (1962).

42. S. Takamura and S. Okuda, J. Phys. Soc. Japan 35, 750 (1973).

43. R. Hanada, S. Takamura, S. Okuda and H. Kimura, Trans. Japan Inst. Met. 11, 434 (1970).

44. P. Vajda and M. Beget, Phys. Stat. Sol. A 23, 251 (1974).

45. J.N. Lomer and R.J. Taylor, Phil. May. 19, 437 (1969).

46. R.R. Coltman Jr., C.E. Klabunde and J.K. Redman, in Fundamental Aspects of Radiation Damage in Metals, edited by M.T. Robinson and F.W. Young (National Technical Information Service, Springfield, VA 1975) pp. 171-190.

47. G. Antesberger, H. Schroeder, K. Sonnenberg and U. Dedek, in Fundamental Aspects of Radiation Damage in Metals, edited by M.T. Robinson and F.W. Young (National Technical Information Service, Springfield, VA 1975) pp. 103-110.

48. H.B. Afman, in Defects in Refractory Metals, edited by R. DeBatist, J. Nihoul and L. Stals (Mol, Belgium, 1971) pp. 310.

49. D.J. Capp, H.W. Evans and B.L. Eyre, J. Less-Common Metals 40, 9 (1975).

50. A. Sosin, in Lattice Defects and Their Interactions, edited by R.R. Hasigutti (Gorden and Breach, 1968) pp. 235-266.